Multiphoton molecular dissociation in intense laser fields

Shaul Mukamel* and Joshua Jortner

Department of Chemistry, Tel-Aviv University, Tel-Aviv, Israel
(Received 15 July 1976)

In this paper we advance a model for multiphoton photofragmentation of an "isolated," collision-free, polyatomic molecule on the ground state potential surface. The molecular energy levels are separated into three regions. In the low energy range the level structure is sparse and only dynamic Stark shifts will be exhibited. In the intermediate energy range the density of bound vibrational states is high and the level structure can be described in terms of mixed (zero-order) states. We argue that in this energy range intrastate anharmonic scrambling may be of central importance in the excitation process, but that intrastate vibrational relaxation and energy redistribution is not encountered for medium-sized molecules. In the high energy region dissociative channels open up and reactive intramolecular decay is handled in terms of resonance theory. The time evolution of a multilevel system, whose highest energy levels are metastable, and which is driven by an intense laser field, is handled by the effective Hamiltonian formalism. Explicit expressions are derived for the photofragmentation yields and their dependence on the molecular parameters and on the field parameters. Specific applications to two distinct model systems are presented. First, we treat the quasidiatomic model, which disregards level scrambling in the intermediate energy range, whereupon near-resonant radiative coupling prevails between the states of a truncated anharmonic oscillator. Second, we have considered the two-ladder model where in the low energy range near-resonant radiative coupling occurs within an anharmonic ladder, while in the intermediate energy range resonant radiative coupling between mixed states prevails. We present numerical simulations of the photofragmentation yields and their dependence on the molecular parameters, such as the diagonal anharmonicity, the molecular dissociation energy, the predissociative widths, and the isotopic shift. We have also explored the dependence of the photofragmentation yields on the pulse parameters, such as the off-resonance energy, the field intensity, and the pulse duration. The quasidiatomic model seems to overestimate the power onset for photodissociation and the power required for the onset of saturation effects, while the two-ladder model is quite adequate to account for the gross features of coherent multiphoton molecular photofragmentation.

I. INTRODUCTION

Laser-induced chemical processes have been under activate investigation during the last five years.[1] Of considerable interest are those processes where laser-induced enhancement of a homogeneous chemical reaction occurs which does not originate from the trivial effects of heating, i.e., increase of the translational temperature of the reactants.[2] Some of the relevant processes induced by laser irradiation in the vibrational molecular spectra in this category are (a) bimolecular reactions between vibrationally excited reactants[1]; (b) vibrational excitation followed by $V-V$ transfer which result in molecular dissociation[3-6]; and (c) multiphoton molecular photodecomposition.[7-14] Processes (a) and (b) can be induced at moderately lower laser powers, while Process (c) requires high power pulsed excitation. Recent experimental work by Abratzumian *et al.*[9,10] and by Robinson and colleagues[11,12] has established that multiphoton photodissociation processes of a variety of molecules, i.e., SiF_4, BCl_3, SF_6, C_2H_4, C_2F_3Cl, CH_3OH, etc., can be induced by a high-power pulsed CO_2 laser, which is characterized by output of ~1–2 J/pulse, pulse duration ~100 nsec, and peak power of 1–5 GW cm^{-2}: The currently available experimental information can be summarized as follows[7-14]:

(1) The photodissociation yield exhibits a sharp power dependence as observed for BCl_3 at moderate power.[13]

(2) The threshold power required to induce observable photofragmentation in SF_6 exceeds ~5 MW cm^{-2}.[11] This threshold power depends, of course, on the sensitivity of the experimental detection system. The onset of field saturation effects, where the photofragmentation yield begins to exhibit a weak field dependence, was observed[14] at a power of 1 GW cm^{-2} for BCl_3.

(3) The photofragmentation is highly isotopically selective. Enrichment factors of ~35 for SF_6 were reported.[9,11]

(4) The photofragmentation yield and the isotope enrichment factor of SF_6 are weakly dependent on the CO_2 laser wavelength.[11]

(5) The isotope enrichment factor and the decomposition yield of SF_6 is a linear function of the number of pulses.[11]

(6) Increasing the pressure of the SF_6/H_2 mixture above 1 torr results in an appreciable reduction of the isotopic enrichment factor.[11]

(7) In some cases, photodissociation was observed under collision-free conditions.[10]

(8) In some systems, such as SF_6, photodissociation occurs to ground state fragments, i.e., $SF_6 \rightarrow SF_5 + F$,[9b,11,12] while in a variety of other systems, dissociation processes, for example of BCl_3, C_2H_4, CH_3OH, C_2F_3Cl, CH_3CN, CH_3OH, CF_2Cl_2, electronically excited photofragments were produced.[10,11,13,14]

(9) The photofragments produced by an infrared high-power laser pulse differ in some cases from those obtained by direct one-photon photodissociation.[10]

Observations (1) and (2) provide strong evidence that the photofragmentation proceeds via a multiphoton pro-

cess of high order. This is compatible with simple minded energetic considerations which imply that the processes $SF_6 \rightarrow SF_5 + F$ and $BCl_3 \rightarrow BCl_2 + Cl$ should be induced by a simultaneous or consecutive absorption of ~25 and of ~31 infrared photons,[15] respectively. One should note that observation (2) might originate from power broadening effects in multiphoton excitation as recently suggested by Bloembergen.[16] Observations (3)–(5) pertaining to isotopic selectivity and time scaling support the notion of a selective laser-induced reaction unaffected by energy scrambling processes, such as $V-V$ transfer, which occur at high pressures [Observation (6)]. Point (7) is central, providing the first experimental evidence for multiphoton photofragmentation of an "isolated" molecule. Finally, Points (8) and (9) are relevant for the elucidation of the nature of the nonradiative decay channel. When ground state photofragments are produced (under collision-free conditions) a possible mechanism involves intramolecular vibrational or rotational predissociation on a single (ground state) potential surface.[17] Production of electronically excited products may result either from direct photodissociation or electronic predissociation on an electronically excited potential surface reached by the multiphoton excitation.

The theoretical understanding of the dissociation of molecules by intense infrared radiation is still in embryonic stages. Rough estimates of multiphoton photodissociation probabilities, which rest on conventional perturbation theory, were provided by Pert,[18] who suggested that such processes will be induced by laser powers ~10^{10} W cm^{-2}. Obviously, at such strong fields the perturbation treatment is inapplicable. Goodman, Stone, and Thiele[19] treated the coherent and incoherent excitation of a harmonic oscillator by a strong radiation field. A similar approach for the incoherent excitation problem, recast in terms of a master equation, was presented by Gordiets *et al.*[5] In the recent work of Goodman, Stone, and Thiele,[19b,c] only level population was considered and intramolecular decay processes were not accounted for, while in the original work of Goodman and Thiele[18a] microscopic unimolecular decay constants were properly assigned to the higher states in the incoherent excitation model, but explicit solutions were provided only for a two-level system. The important role of anharmonicity effects which results in some important quantitative features of the level populations was not taken into account in that work. A recent study of multiphoton excitation of a single molecule which focuses attention on anharmonicity effects as well as on field effects was provided by Bloembergen.[16] This treatment rests on a classical formulation for the excitation of a single anharmonic oscillator with a cubic potential term. Bloembergen's theory assumes that the distribution of the excited molecular levels is Poissonic, as is the case for a harmonic oscillator, while the anharmonicity just affects the energy absorbed by the system. Bloembergen assumed a coherent excitation to a low ($v \simeq 3$–4) level, followed by an efficient intramolecular vibrational energy redistribution, and by a subsequent sequence of one-photon transitions increasing the energy in the quasicontinuum. This last assumption is questionable in view of experimental evidence regarding slow intramolecular vibrational relaxation[20–23] which will be discussed in Sec. II. Bloembergen's model[16] is of considerable interest in providing a clue for the interplay between anharmonicity effects and field effects and in focusing attention on the possible role of intramolecular vibrational relaxation in such processes. The general features of multiphoton photodissociation by intense laser radiation were recently discussed by Abartzumian, Chekalin, Gorokhov, Letokhov, Markov, and Ryabov.[24] They argue, presumably on the basis of perturbation-type calculations, that dynamic Stark broadening effects in laser fields of ~1 GW cm^{-2} cannot explain the photofragmentation process of an anharmonic molecule. They have also considered the possibility of intramolecular vibrational relaxation (i.e., intramolecular $V-V$ transfer) and assert[24] that this process is inefficient. They conclude that "the way how the molecule overcomes the difficulties connected with anharmonicity in vibrational frequencies during the absorption (process) is not clear."[24]

These multiphoton photofragmentation processes constitute a new class of photophysical phenomena. The understanding of these interesting processes requires the elucidation of the following points:

(i) *Diagonal anharmonicity effects.* As only a single vibrational mode of the polyatomic molecule is in near resonance with the electromagnetic field at low energies, one should inquire as to how the anharmonicity of this special mode affects the multiphoton excitation and the level populations.

(ii) *Intrastate scrambling effects.* The description of the level structure of the lowest potential surface of a polyatomic molecule in terms of independent anharmonic oscillators (corresponding to different vibrational modes) is expected to break down at some (as yet unspecified) energy above the electronic origin of the potential surface, in view of intrastate off-diagonal anharmonic coupling between different modes. The special zero-order mode which is in near resonance with the laser field is then mixed with other modes. The physical situation is reminiscent of interstate coupling between vibronic levels corresponding to different (zero-order) electronic configurations which results in a scrambled level structure in "small" molecules[25,26] and is manifested by intramolecular relaxation (i.e., intramolecular $E-V$ transfer) in the statistical limit.[26] Addressing ourselves to the problem at hand, we inquire, what are the effects of intrastate level scrambling between different (zero-order) vibrational states on the multiphoton excitation on the ground state potential surface of a polyatomic molecule.

(iii) *Interstate mixing effects.* As electronically excited photofragments were experimentally detected in some cases of multiphoton photofragmentation,[10] one should consider the effects of interstate nonadiabatic coupling between different electronic configurations. It should be noted, however, that in the present case the relevant zero-order states (corresponding to different electronic configurations) which are effectively coupled

to the radiation field are different from those accessible by one-photon excitation from the ground state,[10] which were previously discussed[25,26] in relation to interstate coupling and intramolecular relaxation in polyatomics. One should inquire in this context what the proper description of the mixing between those relevant zero-order states is.

(iv) *Nature of dissociative channels.* This is a problem common to the description of unimolecular chemical reactions.[27] In the present context it will be interesting to elucidate the nature of the metastable states above dissociation threshold and to handle their decay in terms of resonance theory of unimolecular processes.[27]

(v) *Effects of external perturbations.* Although we shall be concerned here with multiphoton photofragmentation of a single isolated molecule, collisional effects on such processes are of interest. It is well established[1,2] that $V-V$ intermolecular energy transfer may result in excitation to high states and subsequently to dissociation. Such processes (which are not isotopically selective) are of little interest in the present context as they do not provide any new physical features. Collision-induced vibrational and rotational redistribution within a single molecule will drastically affect the nature of the multiphoton photodissociation process via phase shifts (proper T_2 processes), cross relaxation (improper T_2 processes), and even by collision-induced decomposition (T_1 processes). In an isolated molecule coherent multiphoton excitation of the complex level structure (of scrambled states) is exhibited, while in a collisionally perturbed molecule coherence effects will be eroded. A comparison between these two distinct processes will be of interest.

(vi) *Effects of intense electromagnetic field.* Multiphoton molecular photodissociation was observed[7-14] in intense electromagnetic fields (~5 MW cm^{-2}–10 GW cm^{-2}). A theory of this process cannot just consider various features [points (i)–(iv)] of the molecular problem but has to provide a framework for molecular photophysics in intense electromagnetic fields. The following effects are of interest.

(a) *Dynamic Stark shifts.*[28,29] In intense fields, power broadening effects will result in compensation of anharmonicity effects in the special zero-order mode [Point (1)] which is near resonance with the field.

(b) *Saturation effects.* Such phenomena are well known for a two-level system where the time response was treated by Rabi[30] while the line shape was handled by Karplus and Schwinger.[31] A proper theoretical treatment for a multilevel system has to be provided.

(c) *Intrastate and interstate coupling in an intense electromagnetic field.* All previous treatments of anharmonic intrastate coupling and nonradiative relaxation considered excitation by weak electromagnetic fields which do not affect the intramolecular coupling. It is an open question whether intense electromagnetic fields do affect intrastate scrambling, interstate massing, and possibly intramolecular vibrational or electronic relaxation.

In this paper we shall address ourselves to the problem of multiphoton photofragmentation of an isolated molecule on the lowest electronic potential surface. A single molecular mode which (at least for low vibrational quantum numbers) is in near resonance with the laser field will be represented in terms of a truncated anharmonic oscillator. The implications of intrastate coupling and intrastate vibrational relaxation for the excitation process in an intense laser field will be explored. In particular, we shall first treat an anharmonic oscillator driven by an intense laser field. Subsequently, we shall consider the interesting problem of how intrastate coupling can compensate for anharmoncity effects and how it affects the level populations in a strong electromagnetic field. The decay channels for photofragmentation occurring via rotational, vibrational, or electronic predissociation[17] will be described in terms of resonance theory[27] by attributing appropriate decay widths to the highest lying zero-order levels. Next, we shall handle the response of the molecular system to an intense laser field which is near resonance with a sequence of levels, some of which are metastable with respect to decay to dissociative channels. This central issue, which constitutes a generalization of the Rabi two-level problem[30] for a multilevel system, was handled utilizing the effective Hamiltonian formalism[26b,c,32,33] and which was recently advanced by the present authors[34] and by Larsen and Bloembergen[35] for the study of the problem at hand. Numerical studies, based on the effective Hamiltonian formalism, will be presented for the two types of model systems. First, we shall treat a molecule which is optically pumped up a vibrational ladder which corresponds to a single anharmonic mode, exploring the interplay between anharmonicity effects and field effects. Second, we shall handle the case where intrastate anharmonic coupling compensates for anharmonicity defects. Our results will be helpful in elucidating the gross features of multiphoton photodissociation of a single molecule in an intense infrared laser field.

II. MOLECULAR MODEL

A. Zero-order eigenstates and energy levels

We shall consider an isolated polyatomic molecule, such as SF_6, which undergoes multiphoton photodissociation on the lowest, ground state, electronic potential surface. We shall consider first the vibrational level structure, disregarding for the sake of simplicity the rotational degrees of freedom. As we are interested in the vibrational level structure up to high energies, some care must be exercised in defining the vibrational levels. The nuclear Hamiltonian

$$H = T + U(\mathbf{R}_1, \mathbf{R}_2, \ldots, \mathbf{R}_n) \quad , \tag{II.1}$$

where T is the kinetic energy, and V corresponding to the Born–Oppenheimer potential surface is expressed[36-40] in terms of curvilinear instantaneous internal displacement coordinates $\mathbf{R} \equiv (\mathbf{R}_1, \mathbf{R}_2, \ldots)$ which are related to the Cartesian coordinates $\mathbf{X}$ by the nonlinear transformation $\mathbf{R} = \check{\mathbf{B}}\mathbf{X}$, where the tensor $\check{\mathbf{B}}$ has been considered by several authors.[36-41] The zero-order Hamiltonian can be arbitrarily chosen by taking the

potential energy through fourth-order terms in the internal displacement coordinates

$$H_0 = T + U_0 \quad , \tag{II.2}$$

where

$$U_0 = \sum_{i \leq j} K_{ij} \mathbf{R}_i \mathbf{R}_j + \sum_{i \leq j \leq k} K_{ijk} \mathbf{R}_i \mathbf{R}_j \mathbf{R}_k + \sum_{i \leq j \leq k \leq l} K_{ijkl} \mathbf{R}_i \mathbf{R}_j \mathbf{R}_k \mathbf{R}_l \quad .$$

A nonlinear transformation from internal to normal coordinates space results in explicit expressions for the zero-order energy levels. In the absence of Fermi resonances these energy levels are[41]

$$E(\{v_s\}) = \sum_s \omega_s (v_s + g_s/2) + \sum_{s,s'} X_{ss'} (v_s + g_s/2)(v_{s'} + g_{s'}/2) + \sum_{t,t'} X_{tt',tt'} \quad , \tag{II.3}$$

where $\{v_s\} = v_1, v_2, \ldots, v_N$ corresponds to the collection of the vibrational quantum numbers, ω_s are the characteristic frequencies with the degeneracies g_s, the coefficients $X_{ss'}$ denote the anharmonicity constants, while $X_{tt',tt'}$ represent additional contributions of high-order terms which are independent of $\{v_s\}$ together with vibration–rotation coupling. Explicit expressions for these coefficients were derived by Nielsen.[41] Although the zero-order Hamiltonian is sufficient to specify accurately the low lying energy levels, it is not adequate at higher energies where coupling between zero-order states[42] $\{|v_s\rangle\}$ occurs via the perturbation term

$$V_A = U - U_0 \quad . \tag{II.4}$$

V_A corresponds to high-order anharmonic coupling. At this point the attentive reader may argue that one can, in principle, solve the Schrödinger equation with the full Hamiltonian, Eq. (II.1), to obtain the exact nuclear eigenstates and energy levels. This is, obviously, a valid but unpractical argument commonly encountered in theoretical discussions of intramolecular coupling and intramolecular relaxation phenomena. Choosing a "reasonable" zero-order basis set, where (1) the energy levels are close to the exact eigenstates (i.e., level shifts are small), and (2) the perturbation term, Eq. (II.4) in the present case, is sufficiently small to induce only near-resonance intramolecular coupling, has some definite advantages. One can then specify the coupling between the radiation field and the molecular zero-order levels focusing attention only on those zero-order levels which are in near resonance with the radiation field. This conventional approach will enable us to specify the nature of interstate coupling between zero-order states and intramolecular vibrational relaxation on the ground state potential surface.

The vibrational level structure is schematically portrayed in Fig. 1. The laser frequency $\hbar\omega$ is near resonant with a certain manifold of zero-order levels $|v\rangle \equiv |v, 0, 0, 0 \cdots 0\rangle$ characterized by the energies $E(v)$, Eq. (II.4) (e.g., those states containing a dominant contribution from the ν_3 vibrational mode in the case of SF_6). These zero-order states will be characterized by the single vibrational quantum number v. This special subset of zero-order states will be singled out in the present treatment as they provide, at least for sufficiently low values of v, a set of "doorway states" for near-resonance coupling with the radiation field. This subset of levels $\{|v\rangle\}$ are well separated in energy relative to the matrix elements of V_A, Eq. (II.4), which combine these states, i.e., $E(v) - E(v') \gg \langle v | V_A | v' \rangle$ for all $v \neq v'$, so that high-order anharmonic coupling between these zero-order states can be disregarded. The other vibrational states of the molecule can be now described in terms of two alternative basis sets: (a) A set of the anharmonic modes $|\{v_{s'}\}\rangle$, where $\{v_{s'}\} \neq (v, 00000)$, excluding the special mode $|v\rangle$, which are eigenstates of the zero-order nuclear Hamiltonian, Eq. (II.2). These zero-order states are coupled among themselves (as well as to the subset $|v\rangle$) by the high-order anharmonic terms V_A, Eq. (II.4); (b) A prediagonalized basis set $\{|b\rangle\}$, characterized by the energies E_b, which is formed by diagonalizing the total nuclear Ham-

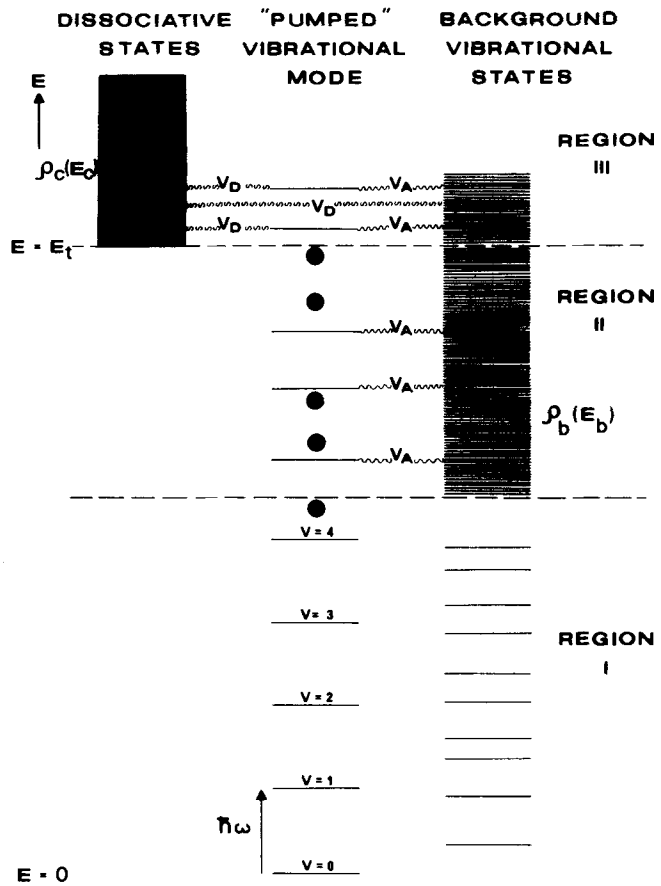

FIG. 1. Molecular energy level structure of a polyatomic molecule. The "special" set of $\{|v\rangle\}$ states is near resonance with the laser energy $\hbar\omega$ at low energies. V_A denotes anharmonic intrastate coupling with the discrete prediagonalized background states $\{|b\rangle\}$ which are characterized by the density of states $\rho_b(E_b)$. V_D represents nonadiabatic coupling of the $\{|v\rangle\}$ and of the $\{|b\rangle\}$ states with the dissociative continuua which are characterized by the density of states ρ_c. The three energy regions I, II, and III are schematically separated by horizontal dashed lines.

TABLE I. Densities of vibronic states in SF_6.[a]

$E(cm^{-1})$	$\rho(states/cm^{-1})$
1 000	0.16
2 000	3
3 000	30
4 000	200
5 000	10^3
10 000	2×10^8
19 000	3×10^{11}

[a]Reference 43.

iltonian, Eq. (II.1), in the basis set $\{|v_{s'}\rangle\}$. The $\{|b\rangle\}$ basis obeys the relations $\langle b|V_A|b'\rangle = 0$ and $V_A(E_b) \equiv \langle b|V_A|v\rangle \neq 0$, whereupon the high-order anharmonic interaction induces coupling only between the special subset $\{|v\rangle\}$ and the background $\{|b\rangle\}$ of other vibrational states. In Fig. 1 we have presented the zero-order states which correspond to the special vibrational ladder $\{|b\rangle\}$. The latter are characterized by the density of states $\rho_b(E_b)$ at the energy E_b above the electronic origin of the ground state.

B. Segregation of energy regions

In a polyatomic molecule we can distinguish three energy regions in the order of increasing energy.

1. Low energy range, bound state, sparse level distribution

For low values of v the density of background states $\rho_b(E_b)$ is low, i.e.,

$$V_A(E_b) \ll [\rho_b(E_b)]^{-1} \quad . \tag{II.5}$$

In this case intrastate scrambling of the $\{|v\rangle\}$ states with the background states is trivially small and the zero-order states $\{|v\rangle\}$ and $\{|b\rangle\}$ are "pure," constituting a good approximation for the eigenstates of the total Hamiltonian, Eq. (II.1). When an intense electromagnetic field is switched on, only power broadening effects, i.e., dynamic Stark shifts,[28,29] will be exhibited.

2. Intermediate energy range, bound states, dense level distribution, mixed states

At higher energies the special subset levels $\{|v\rangle\}$ are quasidegenerate with a background manifold of $\{|b\rangle\}$ states as $\rho_b(E_b)$ increases fast with increasing energy. To provide a rough estimate for the energy dependence of $\rho_b(E_b)$, we assert that $\rho_b(E_b) \sim \rho(E_b)$, where the total density of vibrational states (Table I) is $\rho(E_b) \propto E_b^N$, with N corresponding to the number of vibrational degrees of freedom. When the coupling terms $V_A(E_b)$ exceed the level spacing $\sim \rho_b(E_b)^{-1}$, near-resonance intrastate coupling becomes important. This near-resonance coupling between $\{|v\rangle\}$ and $\{|b\rangle\}$ is distinct from the conventional situation of Fermi, Fermi–Denison, and Coriolis coupling between low lying vibrational states, as in the present case the coupling between nearly degenerate high energy nuclear states is induced by high-order anharmonic terms, Eq. (II.3). The onset of Region II is determined by the condition for effective intrastate coupling

$$V_A(\bar{E}_b)\,\rho_b(\bar{E}_b) > 1 \quad . \tag{II.6}$$

Thus at energies $E > \bar{E}_b$, where $\bar{E}_b$ is determined by Eq. (II.6), the zero-order states of Fig. 1 lose their identity and should be considered in terms of (complicated) superpositions

$$|m\rangle = \sum_v \alpha_v^m |v\rangle + \sum_b \beta_b^m |b\rangle \quad . \tag{II.7}$$

An immediate consequence of level scrambling is the spread of those levels effectively coupled by the radiation field over the energy range $W(E_b) \sim 2\pi |V_A(E_b)|^2 \times \rho_b(E_b)$, as is the case for interstate coupling (between two different electronic configurations) in polyatomic molecules.[25,26] We now inquire what are the general conditions that intrastate coupling will result, in principle, in intramolecular vibrational relaxation. It is now apparent[26] that Condition (II.6) alone is not sufficient to ensure the occurrence of such a process in a discrete level structure. Referring again to studies of the interaction of electronically excited states of large molecules with weak electromagnetic fields, we recall that the necessary conditions[26c] for intramolecular relaxation are as follows: (1) A small number of zero-order states (e.g., the $\{|v\rangle\}$ manifold in the present case) which are well separated in energy are effectively coupled by the radiation field, so that a metastable nonstationary state of the system which exhibits time evolution is selected by the radiative coupling. (2) These zero-order states $\{|v\rangle\}$ interact effectively (via intramolecular coupling) with background states $\{|b\rangle\}$. (3) The background states exhibit an effective sequential decay process. We assume first that Conditions (1) and (2) above are satisfied in Region II. To explore the possibility that Condition (3) also holds, we have to consider the nature of sequential decay processes of the background states $\{|b\rangle\}$ in the isolated molecule. Although the spectrum in this region consists of bound states with respect to fragmentation, we note that, strictly speaking, the levels are metastable, as these states decay by infrared emission. A proper description of such separated decay process will involve the assignment of an infrared decay width γ_b^{ir} to each of the $\{|b\rangle\}$ states, as well as to the states $\{|v\rangle\}$. Typical infrared decay times are $\hbar/\gamma_b^{ir} \sim 10^{-3}$–$10^{-4}$ sec, so that $\gamma_b^{ir} \simeq 10^{-8}$–$10^{-9}$ cm^{-1}. Now, when the level spacing $\rho_b(E_b)^{-1}$ in the $\{|b\rangle\}$ manifold is smaller relative to the width γ_b^{ir} of these levels,

$$\gamma_b^{ir}\,\rho_b(\check{E}_b) > 1 \quad , \tag{II.8}$$

overlap of the background levels is exhibited and the manifold acts as an effective dissipative continuum for intramolecular vibrational relaxation (IVR). Thus, for energies $E \gtrsim \check{E}_b$, where $\check{E}_b$ is determined by Eq. (II.8), IVR can, in principle, occur. It has been shown that for random coupling terms[42] $V_A(E_b)$ the IVR rate, Γ_v^{IVR}, of an "initially excited" $|v\rangle$ level located at $E > \check{E}_b$ is given by the Fermi golden rule,

$$\Gamma_v^{IVR} = 2\pi\,|V_A(E_b)|^2\,\rho_b(E_b) \quad . \tag{II.9}$$

From the available level density data[43] for the ground electronic state of SF_6 (Table I), we assert that Condition (II.8) for the onset of IVR sets in at $\tilde{E}_b = 10^4$ cm^{-1} above the ground state where $\rho_b \gtrsim 10^8$ cm. For energies exceeding 10^4 cm^{-1} above the ground state of SF_6, the necessary condition for the occurrence of IVR is satisfied. To assert whether this process is of any importance (on the time scale of the "lifetime" of the zero-order state), one has to examine the magnitude of Γ_v^{IVR} which, unfortunately, is unknown. Thus, in Region II we have to account for (a) the effects of level scrambling throughout the entire energy range, whereupon a proper description of the energy levels should be given in terms of the mixed $\{|m\rangle\}$ states, Eq. (II.7). We shall return to this problem in Secs. III and VI; (b) The possible effects of IVR in the higher energy range of Region II. The problem of intramolecular vibrational relaxation in an isolated molecule (induced by excitation in weak electromagnetic fields) is not yet well understood. Rice and Nordholm[20a] and Zare *et al.*[20b] have recently considered a variety of recent experimental data in isolated polyatomic molecules such as single vibronic level fluorescence[26c,44] from electronically excited singlet states of benzene, naphthalene, anthracene, and their derivatives, mass spectroscopy,[22] infrared chemiluminescence of medium-sized radicals,[23] and optical excitation of tetracene in molecular beams.[20b] These experiments indicate, at least in some cases, that IVR is slow on the time scale of the lifetimes of the metastable state. On the other hand, Lim and Okajima[45] have presented evidence for efficient IVR in the first excited singlet state of tetracene and pentacene which is faster than 10^{-9} sec. We note in passing that the latter evidence pertains to large molecules, e.g., the pentacene molecule being characterized by 105 vibrational degrees of freedom. As we are concerned here with multiphoton excitation of polyatomic molecules of moderate size (4–7 atom molecules), we shall assume (see Sec. IV) that IVR (and intramolecular vibrational energy redistribution) in these molecules is *slow* relative to the rate of the photofragmentation process which will now be considered.

3. Reactive region, metastable states

At energies above the first dissociative threshold E_t (to ground state or to electronically excited fragments), a dissociative channel opens up. The fragmentation process can occur via rotational predissociation,[17] or more likely by vibrational predissociation.[17] Alternatively, when the ground state and electronically excited potential hypersurfaces do intersect, fragmentation can occur via electronic predissociation.[17] Above the dissociation threshold all the zero-order nuclear states $\{|v\rangle\}$ and $\{|b\rangle\}$ are metastable and can be described in terms of decaying resonances due to coupling to the continuum states $\{|c\rangle\}$ (Fig. 1). An alternative legitimate approach involves the description of those mixed $\{|m\rangle\}$ states, Eq. (II.7), which we located at $E > E_t$ in terms of metastable states. Provided that interference effects between resonances are negligible, we can characterize each metastable state by an appropriate decay width in the spirit of resonance theory of intramolecular decay processes.[27]

Up to this point we have been concerned with the features of the molecular system. We shall now utilize this description to consider possible models for molecular multiphoton photofragmentation.

III. MODELS FOR MULTIPHOTON MOLECULAR PHOTOFRAGMENTATION

We now proceed to consider three distinct models for effective and selective excitation which is accompanied by photofragmentation of an isolated, collision-free molecule by an intense laser field. Each of these models attempts to emphasize different aspects of the molecular level structure which were discussed in the preceding section.

(A) *The unimolecular decomposition model.* This model advanced by Bloembergen[16] envisages multiphoton photodissociation to occur in two steps. The molecule is excited from the ground vibrational state via the anharmonic ladder $\{|v\rangle\}$ in Range I, where field effects compensate for anharmonicity effects. At $v = 3$–4, the vibrational density of states is considered to be sufficiently large and "the vibrational energy will spread out into a quasicontinuum of hot bands."[16] We note in passing that Bloembergen's estimate of the onset of the quasicontinuum, which does not distinguish between intrastate coupling and intramolecular vibrational relaxation in Range II, is somewhat underestimated in view of the density of states data for SF_6 displayed in Table I; however, this is just a minor technical detail. What is central in this model is that the spread of energy among the vibrational modes in Range II involves a complete intrastate vibrational (and rotational) internal energy redistribution, which can be specified by an effective vibrational temperature T^*. T^* is subsequently increased by a sequence of one-photon absorption processes until the photodissociation threshold is reached. The second stage in this model, which assumes effective vibrational energy redistribution in the isolated molecule in Range II, bears a close analogy to the RRKM theory[46] of unimolecular reactions.

(B) *The quasidiatomic model.* This model, proposed by the present authors,[34] asserts that the effects of intramolecular level coupling and intramolecular vibrational relaxation are negligible relative to the dissociation rate and that near-resonant radiation coupling prevails only between adjacent vibrational levels of the special subset $\{|v\rangle\}$ of the zero-order states. The molecule is optically pumped throughout Regions I and II via radiative coupling with the $\{|v\rangle\}$ levels until the reactive region III is reached. Multiphoton photofragmentation is described in terms of truncated anharmonic oscillators, whose upper levels are metastable, which is driven by an intense laser field. A preliminary study of this model system was already provided[34] and detailed numerical results will be presented in Sec. V.

(C) *The two-ladder model.* This model assumes, as in Model (B), that intramolecular vibrational relaxation in Region II is of minor importance and that in contrast

TABLE II. Isotope shifts in the vibrational spectra of some polyatomic molecules.

Molecule		$S(cm^{-1})$
BCl_3	(11/10)	39.0
CF_2Cl_2	(13/12)	32.0
SF_6	(34/32)	17.4
SiF_4	(29/28)	8.9
O_sO_4	(187/192)	1.3

to Model (A) no intramolecular vibrational relaxation and no vibrational energy redistribution occurs. However, in variance with Model (B) an attempt is made to account for level scrambling and radiative coupling between mixed states in Region II. We assume that in Range I near-resonance coupling with the radiation field prevails for the special anharmonic subset of $\{|v\rangle\}$ levels, while in Range II the density of the mixed states $\{|m\rangle\}$, Eq. (II.7), is sufficiently large so that there is always an $|m\rangle$ state in resonance with the radiation field Provided that radiative coupling between those $\{|m\rangle\}$ states is effective, we expect that excitation in Range II will occur by resonance coupling, and level mixing compensates for anharmonicity effects. The molecule is then excited by near-resonance radiative coupling in the first $\{|v\rangle\}$ ladder in Region II up to the reactive Region III. This model will be exposed in detail in Sec. VI.

In Fig. 2 we portray a schematic description of these models for multiphoton photofragmentation. These three models have some common characteristics, but they are also distinct in predicting some of the central physical features of the molecular multiphoton photofragmentation. Consider first the common features of the three models. In all three models the description of radiative coupling in Range I is identical, and field effects, which induce dynamic state shifts, compensate for anharmonicity effects. Isotopic selectivity, for moderately large isotope shifts (Table II), is insured in all three models by the selective near-resonance coupling to one isotopic species in Region I. We now consider three different predictions stemming from the three models. First, in Models (A) and (C), resonance radiative coupling is insured in Regions II and III, while in Model (B) anharmonicity defects are of crucial importance not only in Region I but also in Regions II and III. Thus, higher fields are required to induce photofragmentation in Model (B) relative to Models (A) and (C). Second, Models (A) and (C) predict that diatomic molecules will not be photodissociated by intense laser fields, while in Model (B) such a process can, in principle, occur provided that anharmonicity defects are not too large (see Sec. V). Third, Models (A) and (B) predict that photodissociation will occur on the ground electronic surface. This is obvious for the quasidiatomic model, while for the unimolecular decomposition picture which bears a close analogy to the RRKM model[46] the general rule (with very few exceptions) in unimolecular chemical kinetics is that fragments are produced in their electronic ground state. On the other hand, the two-ladder model [Model (C)] considers effective radiative coupling between adjacent mixed states. We have considered mixed states, Eq. (II.7), which originate from intrastate coupling of zero-order levels of the ground state potential surface. However, mixing between different electronic configurations via nonadiabatic (nuclear kinetic energy and spin–orbit) coupling can result in mixed states which scramble vibronic levels which correspond to different electronic configurations. Thus a conceptually simple extension of the two-ladder model leads to resonance radiative coupling within a second ladder of mixed states which scramble different electronic configurations. This mechanism can result in multiphoton excitation to higher electronic configurations and lead to predissociation into electronically excited photofragments.

We prefer the two-ladder Model (C) to Bloembergen's unimolecular model [Model (A)] because of the following considerations: (a) The assumption of intrastate vibrational equilibrium in an isolated medium-sized molecule (such as SF_6 or BCl_3) which is inherent in Model (A) is questionable in view of a variety of experimental data[19,20,22,23,44] reviewed in Sec. II. (b) Model (A) predicts that the dominating decay channel will result in most cases in fragments in their electronically ground state, in contrast to the prediction of Model (C), which provides a variety of decay channels for the production of fragments in their ground state, in electronically excited states and even for ionic fragments. The latter qualitative consideration is in accord with recent experimental results where in most cases of molecular multiphoton photofragmentation electronically excited radicals were observed.[10] To study Model (C) we have to extend the well known two-level Rabi problem[30] for near-resonance coupling with a manifold of discrete and metastable levels. Model (B) is amenable to theoretical study by the same formalism. We shall now proceed to provide a theoretical framework for the study of Models (B) and (C).

IV. TIME EVOLUTION OF A MULTILEVEL SYSTEM IN AN INTENSE FIELD

We shall now consider the time evolution of a multilevel system, whose highest lying levels are mestable with respect to predissociation, which is driven by an intense laser field. The molecular model is characterized as follows. There are M molecular levels $\{|\alpha\rangle\}$ characterized by the molecular energies $E_\alpha(\alpha = 1, 2 \cdots M)$ which are in near resonance with the laser energy $\hbar\omega$. In the quasidiatomic model of Sec. III, these M molecular levels constitute a truncated anharmonic oscillator, while for the two-ladder model of Sec. III the $N_I(\alpha = 1 \cdots N_I)$ levels in Range I correspond again to the states of an anharmonic oscillator, while the $N_{II} = M - N_I$ $(\alpha = N_I + 1 \cdots M)$ levels in Ranges II and III correspond to the mixed states $\{|m\rangle\}$, Eq. (II.7). The high lying molecular levels in Range III are metastable with respect to predissociation into fragments. The predissociation process can be described in terms of the nonadiabatic coupling with the continuum levels. To each of the states in Range III, located at $E > E_t$ (which will be labeled by $|\bar{\alpha}\rangle$), we assign a decay width,

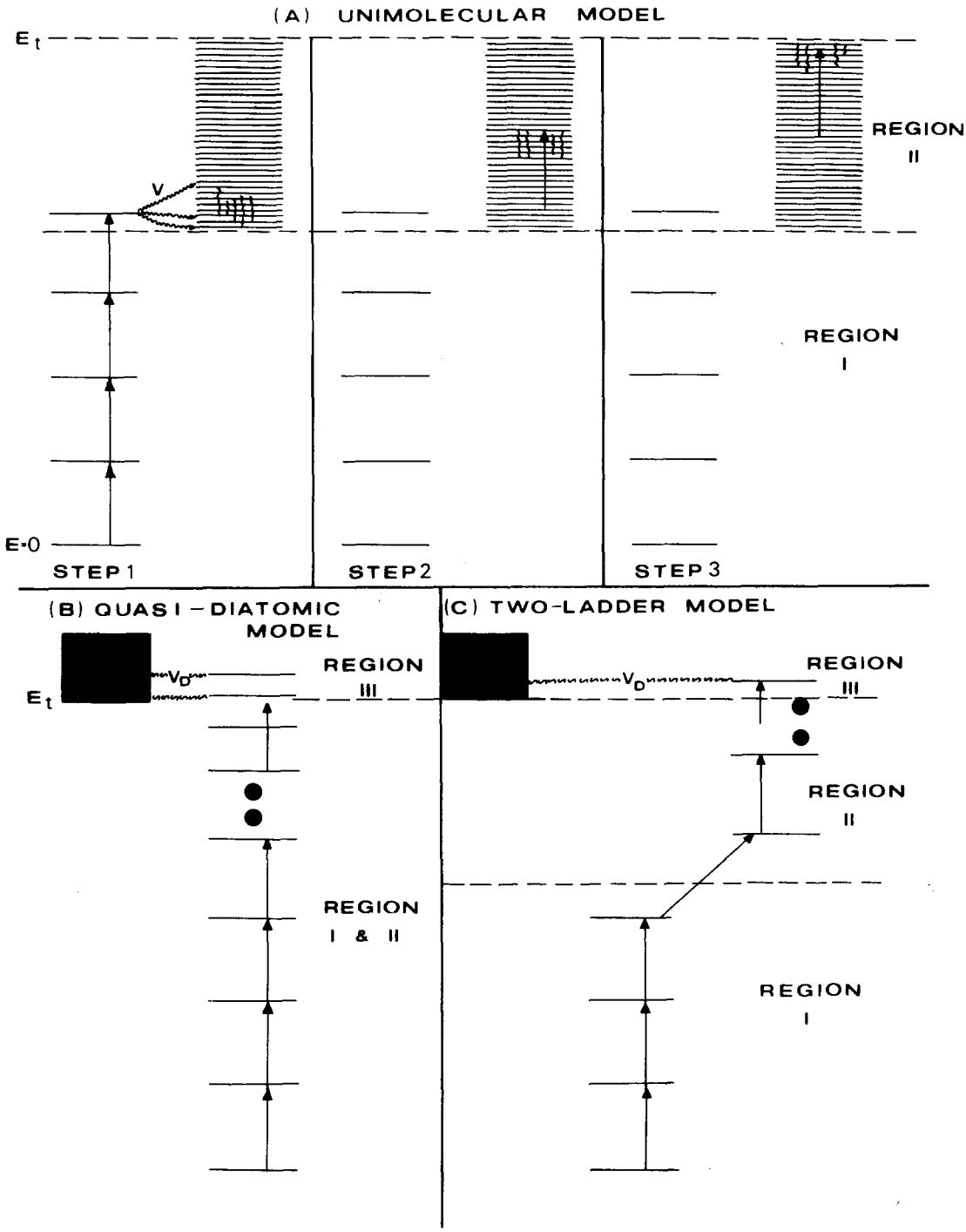

FIG. 2. A schematic representation of three models for multiphoton molecular photodissociation. (A) The unimolecular model (Ref. 16). The molecule is pumped via near-resonance coupling in region I (Step 1) until high density of background states permits intramolecular vibrational relaxation and effective intramolecular vibrational energy redistribution via the anharmonic coupling V_A. After the molecule has acted as its own heat bath a set of sequential one-photon excitation processes (Steps 2, 3, etc.) takes place until the threshold E_t for dissociation is reached. (B) The quasidiatomic model. Intramolecular anharmonic coupling and IVR in Regions II and III are disregarded. The molecule is optically excited via near-resonance coupling between adjacent $\{|v\rangle\}$ states until the metastable states in Region III are reached. (C) The two-ladder model. Intrastate anharmonic coupling and level scrambling in Range II is crucial and the $\{|v\rangle\}$ states in Region II and III lose their identity, IVR is not considered, but rather effective-resonance coupling between mixed $\{|m\rangle\}$ states is assumed to occur in Regions II and III. The molecule is excited by near-resonance coupling between $\{|v\rangle\}$ states in Region I and via resonance coupling between $\{|m\rangle\}$ states in Regions II and III, until metastable $|m\rangle$ states are reached.

$$\Gamma_{\bar{\alpha}}^{D} = 2\pi \left|\langle \bar{\alpha}| V_D |c\bar{\alpha}\rangle\right|^2 \rho_{c\bar{\alpha}} \ , \qquad \text{(IV.1)}$$

where V_D is the nonadiabatic coupling, $\{|c\bar{\alpha}\rangle\}$ are the continuum dissociative states coupled to the state $|\bar{\alpha}\rangle$, while $\rho_{c\bar{\alpha}}$ corresponds to the density of states in the dissociative continuum. Assuming that the spacing between resonances originating from zero-order states which decay into a common decay channel considerably

exceeds their decay widths, Eq. (IV.1), the width Γ_{α}^{D} represents the fragmentation rate of the state $|\bar{\alpha}\rangle$.

Next, we turn to consider the laser field. We specify the intense electromagnetic field in terms of a state $|n\rangle$ containing n photons ($n \gg 1$) of frequency ω in a single mode, which is switched on the time scale $0 \leq t \leq T$. We note in passing that the results for $n \gg 1$ (or more accurately $n \gg M$) derived using the quantum description of the radiation field are equivalent to those obtained using a classical field. The off-resonance energy Δ for the first molecular transition is

$$\Delta = E_2 - E_1 - \omega \tag{IV.2}$$

(where we use the units $\hbar = c = 1$). Provided that all the off-resonance energies ($E_{\alpha} - E_{\alpha-1} - \omega$) are not too large, we can safely assume that only adjacent states are coupled by the radiative interaction $H_{\rm int} = \mu \cdot \epsilon$, where μ is the dipole operator and ϵ corresponds to the electrical field, whereupon

$$\langle \alpha, n' | H_{\rm int} | \alpha', n'' \rangle = \delta_{n'', n'\pm 1} [\mu_{\alpha', \alpha+1} \epsilon \delta_{\alpha', \alpha-1} + \mu_{\alpha, \alpha-1} \epsilon \delta_{\alpha', \alpha+1}] \ . \tag{IV.3}$$

The combined zero-order states $|\alpha, n'\rangle$ of the molecule and the radiation field, i.e., the "dressed" molecular states, are characterized by the energies

$$E(\alpha, n') = n'\omega + E_{\alpha} \ . \tag{IV.4}$$

Let us now consider a group of near-resonant dressed molecular states $|1, n\rangle$, $|2, n-1\rangle \cdots |\alpha, n-\alpha+1\rangle$ which correspond to the energetic sequence

$$E(\alpha, n-\alpha+1) = n\omega + E_{\alpha} - (\alpha - 1)\omega; \quad \alpha = 1 \cdots M \ . \tag{IV.5}$$

These dressed states are radiatively coupled according to Eq. (IV.3). Now, the laser frequency ω is of the order of the spacing between adjacent molecular levels, whereupon the energetic spread δ of the dressed states, Eq. (IV.5), is

$$\delta \ll \omega \ . \tag{IV.6a}$$

Furthermore, the laser frequency considerably exceeds the radiative coupling terms

$$\mu_{\alpha, \alpha+1} \epsilon \ll \omega, \quad \alpha = 1 \cdots M \ . \tag{IV.6b}$$

Conditions (IV.6a) and (IV.6b) permit us to neglect off-resonance radiative coupling between sets $|\alpha, n-\alpha+1\rangle$ and $|\alpha, n'-\alpha+1\rangle$ where $n' \neq n$. This amounts to invoking the rotating-wave approximation.[47] Finally, to complete the list of approximations we shall neglect spontaneous infrared emission which predominantly occurs between adjacent levels (i.e., $\alpha \to \alpha - 1$). Incorporation of the effects of spontaneous emission in intense electromagnetic fields will introduce interesting cascading effects.[48] However, the infrared decay times are $(\gamma^{\rm ir})^{-1} \sim 10^{-3}$–$10^{-4}$ sec, which are considerably longer than the relevant time scale with which we are concerned here, i.e., $(\Gamma_{\bar{\alpha}}^{D})^{-1} \simeq 10^{-12}$–$10^{-9}$ sec for the decay of metastable states and $T \simeq 10^{-9}$–10^{-7} sec for the duration of the pulse. We thus assert that the effects of spontaneous infrared emission can be quite safely neglected.

We are now concerned with the time evolution of a system which is characterized by a fine number of discrete dressed molecular states $|\alpha, n-\alpha+1\rangle$ ($\alpha = 1 \cdots M$, $n \gg M$) as well as by several (dressed) intramolecular continuua $\{|c\bar{\alpha}, n-\bar{\alpha}+1\rangle\}$ (degenerate with the $\bar{\alpha}$ states in Range III). This problem can be handled by the effective Hamiltonian formalism, which was utilized for the study of electronic intramolecular relaxation and photon scattering from a complex molecular level structure[26b,c] and which will be now briefly considered. The Hilbert space is partitioned as follows:

$$\hat{P} = \sum_{\alpha=1}^{M} |\alpha, n-\alpha+1\rangle\langle\alpha, n-\alpha+1| \ ,$$

$$\hat{Q} = \sum_{\bar{\alpha}} \int dE_{c\bar{\alpha}} \rho_{c\bar{\alpha}} |c\bar{\alpha}, n-\bar{\alpha}+1\rangle\langle c\bar{\alpha}, n-\bar{\alpha}+1| \ ,$$

$$\hat{P} + \hat{Q} = 1 \tag{IV.7}$$

The time evolution operator $U(t, 0)$ within the $\hat{P}$ subspace spanned by the M discrete (zero-order) levels is given by

$$\langle a | \hat{P} U(t, 0) \hat{P} | a' \rangle = -(2\pi i)^{-1} \int_{-\infty}^{\infty} dE \exp(-iEt) \langle a | \hat{P} G(E) \hat{P} | a' \rangle \ , \tag{IV.8}$$

where the states $|a\rangle$ and $|a'\rangle$ belong to the subspace $\hat{P}$. The Green's function $G(E)$ within the $\hat{P}$ subspace is

$$\langle a | \hat{P} G(E) \hat{P} | a' \rangle = \langle a | (E - H_{\rm eff})^{-1} | a' \rangle \tag{IV.9}$$

being defined in terms of the effective Hamiltonian $H_{\rm eff}$, which for the problem at hand consists of an $M \times M$ complex symmetric matrix

$$H_{\rm eff} = \begin{pmatrix} \text{Regions I and II} & & & & \text{Region III} \\ E(1) & \mu_{12}\epsilon & & 0 & \\ \mu_{21}\epsilon & E(2) & \mu_{23}\epsilon & & 0 \\ & \mu_{32}\epsilon & E(3) & & \\ 0 & & & & \\ & 0 & & [E(M-1) - \tfrac{1}{2} i \Gamma_{M-1}^{D}] & \mu_{M-1,M}\epsilon \\ & & & \mu_{M,M-1}\epsilon & [E(M) - \tfrac{1}{2} i \Gamma_{M}^{D}] \end{pmatrix} , \tag{IV.10}$$

where $E(\alpha) \equiv E(\alpha, n-\alpha+1)$ which is given by Eq. (IV.5). Equation (IV.10) specifies the effective Hamiltonian for the time $0 \leq t \leq T$, when the laser pulse is switched on. For $t > T$ we have to set $\epsilon = 0$ in Eq. (IV.10). The initial state of the system is $|1, n\rangle$ and the probability amplitude for the population of a dissociative state $|\bar{\alpha}\rangle$ in Range III, i.e., the state $|\bar{\alpha}, m-\bar{\alpha}+1\rangle$, at time t is given in terms of Eqs. (IV.8) and (IV.9),

$$C_{\bar{\alpha}}(t) = \langle 1, n | \hat{P} U(t, 0) \hat{P} | \bar{\alpha}, n-\bar{\alpha}+1 \rangle = -(2\pi i)^{-1} \int_{-\infty}^{\infty} dE \exp(-iEt) \times \langle 1, n | (E - H_{\rm eff})^{-1} | \bar{\alpha}, n-\bar{\alpha}+1 \rangle \ . \tag{IV.11}$$

To derive an explicit expression for the yield of multiphoton photofragmentation we shall consider first the probability for the (partial) predissociation yield from the $|\bar{\alpha}\rangle$ state. This probability for dissociation in the time interval $0 \cdots t$ during the pulse is given by

$$P_{1\bar{\alpha}}(t) = \Gamma^D_{\bar{\alpha}} \int_0^t d\tau \, |C_{\bar{\alpha}}(\tau)|^2; \quad 0 \leq t \leq T \ , \tag{IV.12a}$$

while after termination of the pulse the contribution to the dissociation yield from the $|\bar{\alpha}\rangle$ state on the time scale $T \cdots t$ is

$$P_{2\bar{\alpha}}(t) = \Gamma^D_{\bar{\alpha}} \int_T^t d\tau \, |C_{\bar{\alpha}}(\tau)|^2, \quad t > T \ . \tag{IV.12b}$$

The total probability for photofragmentation on the time scale $0 < t < T$ and $t > T$ is obtained by summing up Eqs. (IV.12a) and (IV.12b) over all the metastable states in Range III. For the dissociation probability during the pulse we get

$$P_1(t) = \sum_{\bar{\alpha}} P_{1\bar{\alpha}}(t), \quad 0 \leq t \leq T \ , \tag{IV.13a}$$

while the total dissociation probability after termination of the pulse is

$$P_2(t) = \sum_{\bar{\alpha}} P_{2\bar{\alpha}}(t), \quad t > T \ . \tag{IV.13b}$$

The total photofragmentation yield during the pulse is

$$P_D(T) = P_1(T) \tag{IV.14a}$$

and the total photofragmentation yield is given by

$$P_D = P_1(T) + P_2(\infty) \ . \tag{IV.14b}$$

The Green's function which determines the probability amplitudes, Eq. (IV.11), can be evaluated by standard techniques.[26b,c,32,33] The effective Hamiltonian, Eq. (IV.10), is diagonalized by an orthogonal transformation **D**,

$$\mathbf{D} H_{eff} \mathbf{D}^{-1} = \Lambda \ , \tag{IV.15a}$$

where

$$\Lambda_{jj'} = (\epsilon_j - \tfrac{1}{2} i \gamma_j) \delta_{jj'} \ . \tag{IV.15b}$$

We note in passing that these complex eigenvalues satisfy the diagonal sum rule

$$\sum_{\alpha=1}^{M} E(\alpha) = \sum_{j=1}^{M} \epsilon_j \ , \tag{IV.16a}$$

$$\sum_{\bar{\alpha}} \Gamma^D_{\bar{\alpha}} = \sum_{j=1}^{M} \gamma_j \ . \tag{IV.16b}$$

Equation (IV.16b) implies that the decay widths of the zero-order states in Range III are now spread over all the "new states." The new nonorthogonal basis set $\{|j\rangle\}$ generated by the transformation **D** is characterized by the energies $\{\epsilon_j\}$ and by the widths $\{\gamma_j\}$, which specify these "independently decaying levels." The time evolution operator and the Green's function are in general given by

$$\langle a | \hat{P} G(E) \hat{P} | a' \rangle = \sum_j \frac{\langle a | j \rangle \langle \bar{j} | a' \rangle}{E - \epsilon_j + \frac{1}{2} i \gamma_j} \ ,$$

$$\langle a | \hat{P} U(t, 0) \hat{P} | a' \rangle = \sum_j \langle a | j \rangle \langle \bar{j} | a' \rangle \otimes \exp[-i\epsilon_j t - (\gamma_j t/2)] \ , \tag{IV.17}$$

where $\{|\bar{j}\rangle\} = (\mathbf{D}^{-1})^{\dagger} \{|\alpha, m - \alpha + 1\rangle\}$ is the basis which is complementary to $\{|j\rangle\}$. In the present case the basis set $|\alpha, n - \alpha + 1\rangle$ has a real representation, $\{|j\rangle\} = \{|j^*\rangle\}$, and we get

$$\langle a | \hat{P} G(E) \hat{P} | a' \rangle = \sum_j \frac{\langle a | j \rangle \langle a' | j \rangle}{E - \epsilon_j + \frac{1}{2} i \gamma_j} \ ,$$

$$\langle a | \hat{P} U(t, 0) \hat{P} | a' \rangle = \sum_j \langle a | j \rangle \langle a' | j \rangle \otimes \exp[-i\epsilon_j t - (\gamma_j t/2)] \ . \tag{IV.18}$$

Utilizing Eqs. (IV.10) and (IV.18), the probability amplitude, Eq. (IV.11), can be expressed in the explicit form

$$C_{\bar{\alpha}}(t) = 0, \quad t < 0 \ ,$$

$$C_{\bar{\alpha}}(t) = \sum_j \langle \bar{\alpha}, n - \bar{\alpha} + 1 | j \rangle \langle 1, n | j \rangle \otimes \exp[-i\epsilon_j t - (\gamma_j t/2)], \quad 0 \leq t \leq T \ ,$$

$$C_{\bar{\alpha}}(t) = C_{\bar{\alpha}}(T) \exp[-iE_{\bar{\alpha}}(t - T) - \Gamma^D_{\bar{\alpha}}(t - T)/2], \quad t > T \ . \tag{IV.19}$$

The partial transition probability, Eq. (IV.12), can be now expressed by making use of Eq. (IV.19),

$$P_{1\bar{\alpha}}(t) = \Gamma^D_{\bar{\alpha}} \sum_j \sum_{j'} \langle \bar{\alpha}, n - \bar{\alpha} + 1 | j \rangle \langle 1, n | j \rangle \otimes \langle j' | \bar{\alpha}, n - \bar{\alpha} + 1 \rangle \langle j' | 1, n \rangle \left\{ \frac{1 - \exp[-i(\epsilon_j - \epsilon_{j'}) t - (\gamma_j + \gamma_{j'})(t/2)]}{i(\epsilon_j - \epsilon_{j'}) + [(\gamma_j + \gamma_{j'})/2]} \right\}, \quad 0 \leq t \leq T \ , \tag{IV.20a}$$

$$P_{2\bar{\alpha}}(t) = \left| \sum_j \langle \bar{\alpha}, n - \bar{\alpha} + 1 | j \rangle \langle 1, n | j \rangle \exp[-i\epsilon_j T - (\gamma_j T/2)] \right|^2 \{1 - \exp[\Gamma^D_{\bar{\alpha}}(t - T)]\}, \quad t > T \ . \tag{IV.20b}$$

We have derived a general solution of the problem of coherent excitation and photodissociation of a multilevel system. All that is required is to specify the effective Hamiltonian, Eq. (IV.10), to find its (complex) eigenvalues and eigenvectors according to the recipe given by Eq. (IV.15), and to obtain explicit results for the partial transition probabilities, Eq. (IV.20). Some remarks are now in order:

(a) The general result obtained herein provides a generalization of some well-known results. Thus for a one-level system, $M = 1$, Eq. (IV.20), is nothing but the Fermi golden rule $P(t) = \exp(-\Gamma^D t)$, while for a two-level system Eq. (IV.10) takes the form

$$H_{eff} = \begin{pmatrix} E(1) & \mu_{12}\epsilon \\ \mu_{21}\epsilon & [E(2) - \frac{1}{2} i \Gamma_2^D] \end{pmatrix} ,$$

which is just the Rabi two-level problem[30] which incorporates an additional decay channel. Our solution constitutes a generalization of the Rabi result for a multilevel system.

(b) The solution, Eq. (IV.20), for the multilevel system is oscillatory in time, as is the case for the well-known two-level solution.[30] A sufficient condition for damping of the time oscillations is

$$[(\gamma_j + \gamma_{j'})/2] \gg |\epsilon_j - \epsilon_{j'}| \qquad \text{(IV.21)}$$

for all j and j', whereupon the decay processes will smear out the interference effects. In a multilevel system destructive interference effects between various energy levels ϵ_j which are unevenly spaced will smear out the oscillations. In actual numerical calculations, when Condition (IV.21) was not obeyed, the fragmentation probability, Eq. (IV.20), was averaged over a time interval of $T/100$. Such an averaging process does not just involve a mathematical procedure, as in a real experiment these oscillations are averaged by the finite rise and fall times of the pulse.

(c) At low fields when the off-diagonal matrix elements of the effective Hamiltonian, Eq. (IV.10), are small relative to the level spacing, i.e.,

$$\mu_{\alpha,\alpha'}\epsilon \ll |E(\alpha) - E(\alpha') - \tfrac{1}{2} i(\Gamma_\alpha^D - \Gamma_{\alpha'}^D)| \qquad \text{(IV.22)}$$

for all α, and a perturbative solution is adequate, the photodissociation probability is then proportional to $\epsilon^{2\bar{\alpha}}$, i.e., to the $\bar{\alpha}$th power of the intensity, as expected, for a high-order multiphoton process.

(d) The perturbation treatment will break down when

$$\mu_{\alpha,\alpha'}\epsilon \gtrsim |E(\alpha) - E(\alpha') - \tfrac{1}{2} i(\Gamma_\alpha^D - \Gamma_{\alpha'}^D)| \qquad \text{(IV.23)}$$

for some α and α', and saturation effects will be exhibited. To provide some criteria for saturation effects in a multilevel system we shall first discuss the onset of saturation and subsequently consider the situation of complete saturation. When the radiative coupling terms exceed the spacings and the differences in widths between adjacent levels, i.e.,

$$[\mu_{\alpha,\alpha\pm1}\epsilon]_{OS} \gtrsim |E(\alpha) - E(\alpha \pm 1)| \ , \qquad \text{(IV.24)}$$

$$[\mu_{\alpha,\alpha\pm1}\epsilon]_{OS} \gtrsim |\Gamma_\alpha^D - \Gamma_{\alpha\pm1}^D| \qquad \text{(IV.25)}$$

for all α, the onset of saturation effects {denoted by $[\mu_{\alpha,\alpha\pm1}\epsilon]_{OS}$ in Eq. (IV.24)} will set in, and in contrast to the low field behavior [discussed in Sec. (c)] P_D vs ϵ now exhibits a weak field dependence. At even higher fields when the radiative coupling exceeds the total energetic spread and the widths of the dressed states

$$[\mu_{\alpha,\alpha\pm1}\epsilon]_{CS} \gtrsim \delta \ , \qquad [\mu_{\alpha,\alpha\pm1}\epsilon]_{CS} \gtrsim \Gamma_\alpha^D \qquad \text{(IV.26)}$$

for all α, complete saturation (denoted by $[\mu_{\alpha,\alpha\pm1}\epsilon]_{CS}$) will set in and P_D is expected to be independent of ϵ.

(e) Finally, it is worthwhile to note that the present study provides an adequate treatment not only of field effects but also of the intramolecular (indirect) fragmentation process. This complete treatment yields explicit expressions for the decay probability during the pulse, Eq. (IV.20a), while in some previous work,[19b,c] which did not explicitly incorporate the dissociation process, only the contribution for $t > T$ was considered, resulting in the relation $P_D = \sum_{\bar{\alpha}} |C_{\bar{\alpha}}(T)|^2$ for the photofragmentation yield.

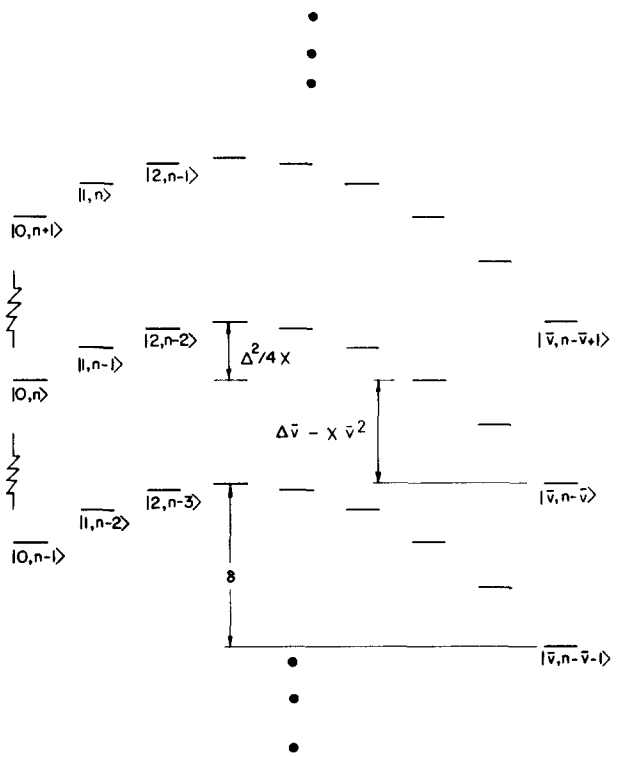

FIG. 3. Combined $|v,n'\rangle$ zero-order states of the molecule and the radiation field.

V. THE QUASIDIATOMIC MODEL

In this model [Model (B), Sec. III] we approximate the relevant molecular levels, which are in near resonance with the laser energy $\hbar\omega$, in terms of a truncated anharmonic oscillator.[34] The molecular energy levels of the state $|\alpha\rangle \equiv |v+1\rangle$ are

$$E_v = \omega_0 v - x v^2 \ , \qquad \text{(V.1)}$$

where ω_0 is the oscillator frequency and x the (diagonal) anharmonicity constant. The discrete (zero-order) spectrum is characterized by $M = \bar{v} + 1$ zero-order states. The dressed molecular states $|v,n'\rangle$, portrayed in Fig. 3, are characterized by the energy levels

$$E(v,n') = n'\omega + v\omega_0 - x v^2 \ , \qquad \text{(V.2)}$$

while a group of near-resonant dressed states (Fig. 4) corresponding to the sequence $|v,n-v\rangle$ is obtained from Eqs. (IV.5) and (V.2) in the form

$$E(v,n-v) = n\omega + v\Delta - v^2 x \ , \quad v = 0,1,\ldots,\bar{v} \ , \qquad \text{(V.3)}$$

where the off-resonance energy, Eq. (IV.2), is

$$\Delta = \omega_0 - \omega \ . \qquad \text{(V.4)}$$

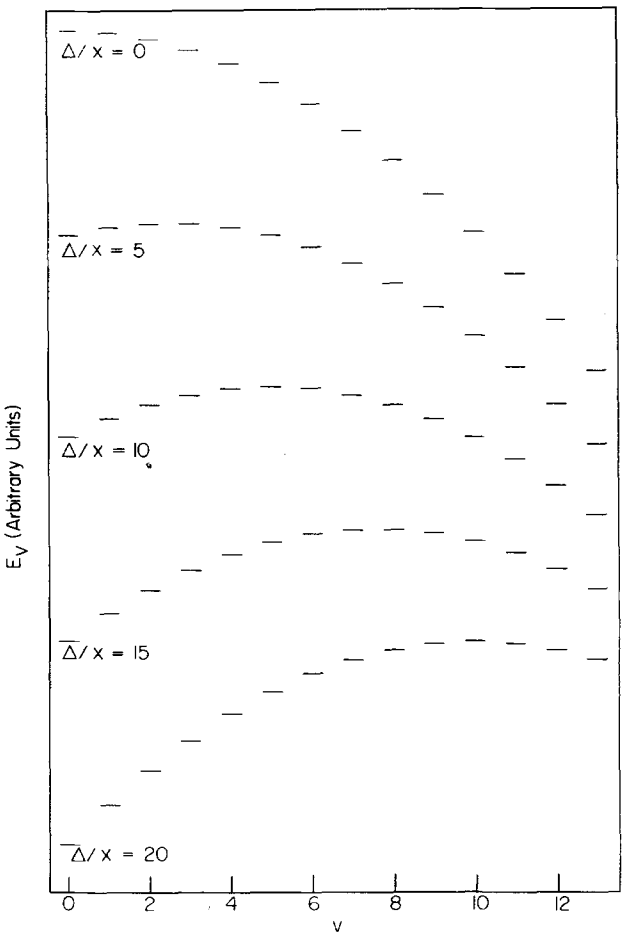

FIG. 4. The zero-order dressed states in the quasidiatomic model for several values of Δ/x.

The energetic spread δ of these latter states, Fig. 3, for a given value of Δ is

$$\delta(\Delta) = (\Delta^2/4x) + x\bar{v}^2 - \bar{v}\Delta \ , \quad \bar{v} \geq \Delta/x \ ,$$
$$\delta(\Delta) = \Delta^2/4x \quad \bar{v} \leq \Delta/x \ . \tag{V.5}$$

Decomposition in this model system is described by assigning a single molecular state $|\bar{v}\rangle$ to Range III, which is characterized by the predissociation width $\Gamma^D_{\bar{v}}$. We could have easily incorporated several metastable states (i.e., $|\bar{v}\rangle$, $|\bar{v}-1\rangle$, ..., etc.) in the reactive region; region; however, in view of lack of microscopic information regarding the decay widths there is little point in doing so. Finally, the radiative coupling, Eq. (IV.3), between adjacent levels is approximated in terms of radiative coupling for a harmonic oscillator,

$$\langle v', n' | H_{\rm int} | v, n\rangle = \mu_{01}\epsilon\delta_{n',n\pm1} \otimes [(v+1)^{1/2}\delta_{v',v-1} + v^{1/2}\delta_{v',v+1}] \ , \tag{V.6}$$

where μ_{01} corresponds to the transition moment for the $v=0 \rightarrow v=1$ transition and where we have assumed n to be a large number.

The effective Hamiltonian, Eq. (IV.10), is characterized by the diagonal matrix elements

$$\langle v, n-v | H_{\rm eff} | v, n-v\rangle = E(v, n-v) \ , \quad 0 \leq v < \bar{v}$$
$$= E(\bar{v}, n-\bar{v}) - \tfrac{1}{2} i \Gamma^D_{\bar{v}} , \quad v = \bar{v} \ , \tag{V.7a}$$

which we expressed in terms of Eq. (V.3), while the off-diagonal matrix elements

$$\langle v, n-v | H_{\rm eff} | v', n-v'\rangle = \langle v, n-v | H_{\rm int} | v', n-v'\rangle \tag{V.7b}$$

are given by Eq. (V.6). Diagonalization of this effective Hamiltonian, Eq. (V.7), results in the complex eigenvalues $\epsilon_j - \frac{1}{2} i\gamma_j$ and the (nonorthogonal) eigenvectors $\{|j\rangle\}$.

The photofragmentation yields, Eq. (IV.20), are now expressed in the form

$$P_1(t) = \Gamma^D_{\bar{v}} \int_0^t |C_{\bar{v}}(\tau)|^2 d\tau \ , \quad 0 \leq t \leq T \ ,$$
$$P_2(t) = |C_{\bar{v}}(T)|^2 \{1 - \exp[-\Gamma^D_{\bar{v}}(t-T)]\} \ , \quad t > T \ . \tag{V.8}$$

Explicit expressions for these yields can be now obtained from Eq. (V.8) together with Eq. (IV.19).

Numerical simulations for the quasidiatomic model were conducted by using the following molecular parameters: the number of vibrational levels was taken to be $M=10$, 15, and 20; the molecular anharmonicity was chosen in the range $x=0-5$ cm^{-1}; the off-resonance energy was varied over the region $\Delta=-50$ cm^{-1} to $+50$ cm^{-1}; and the predissociation width was chosen in the range $\Gamma^D_{\bar{v}}=10^{-5}$ to 10^{-1} cm^{-1}. The pulse duration was taken in the region $T=10-10^4$ nsec, while the field intensity, characterized in terms of the Rabi frequency

$$\omega_R = \mu_{01}\epsilon/\hbar \ , \tag{V.9}$$

was chosen in the range $\omega_R=0.01-10$ cm^{-1}. We note in passing that such laser fields are experimentally accessible, as for a laser power of 1 GW cm^{-2} $\epsilon=10^6$ V cm^{-1}, so that for a typical infrared transition moment of $\mu_{01}=0.1$ D we then have $\omega_R \equiv 2$ cm^{-1}.

Numerical calculations have been performed for the photofragmentation yield $P_1(T)$ during the pulse over the time scale $t=0-T$ and for the yield after termination of the pulse $P_2(\infty)$ occurring during the time interval $t=T-\infty$. We note that the physical system is characterized by frequencies $|\epsilon_j - \epsilon_{j'}| > 10^{12}$ sec^{-1}, whereupon $P_1(T)$ and $P_2(\infty)$ were averaged over the time intervals of $\Delta t=0.3$ nsec.

In Fig. 5 we present the results of model calculations of the molecular dissociation probabilities $P_1(T)$ and $P_2(\infty)$ as a function of the pulse duration at a constant pulse power, while complementary information is obtained from the dependence of $P_1(T)$ and of $P_2(\infty)$ on the predissociative width $\Gamma^D_{\bar{v}}$ at constant T (Fig. 6). At low values of $\Gamma^D_{\bar{v}} T$ the dominating contribution to the photofragmentation yield occurs at times $t > T$ after the pulse is switched off, while for $\Gamma^D_{\bar{v}} T \gg 1$ the dominating contribution to predissociation occurs during the pulse. We also note that for large values of $\Gamma^D_{\bar{v}} T$, $P_1(T) \propto T$ and $P_1(T) \propto \Gamma^D_{\bar{v}}$, while $P_2(\infty)$ is constant, which implies that the system is in a steady state. For even larger values of $\Gamma^d_{\bar{v}} T$, depletion of the ground state ($v=0$) causes deviation from the steady state behavior.

Next, we turn to numerical simulations of anharmonicity effects and field saturation effects in this model

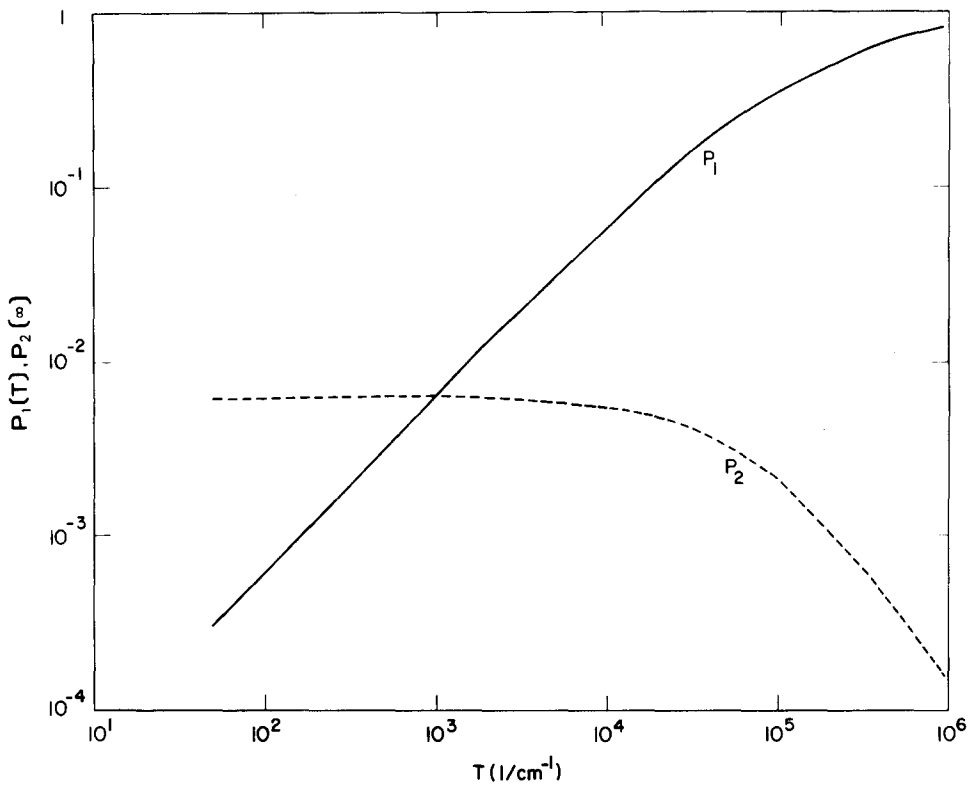

FIG. 5. The dependence of the molecular dissociation probability during the pulse $P_1(T)$, and of the photofragmentation probability after the pulse, $P_2(\infty)$, on the pulse duration T. Calculations for the quasidiatomic model with the parameters $M=10$, $\omega_R=10\ \mathrm{cm}^{-1}$, $x=1\ \mathrm{cm}^{-1}$, $\Delta=0$, $\Gamma_{\bar{v}}^{D}=10^{-3}\ \mathrm{cm}^{-1}$.

system, which were conducted for $\Gamma_{\bar{v}}^{d}T=5$ where photofragmentation occurs predominantly during the pulse and $P_D\simeq P_1(T)$. Some of the features of the field dependence are displayed in Figs. 7(a) and 7(b), where we portray P_D vs the laser frequency (expressed in terms of Δ) at various values of ω_R, for $M=10$ and for $M=15$. Additional information concerning the dependence of the photofragmentation yield on the number M of the discrete quasidiatomic levels is portrayed in Fig. 8. Finally, in Fig. 9 we explore anharmonicity effects displaying $P_1(T)$ vs Δ for various values of x. Several features of these numerical results should be noted:

(1) At low fields P_D increases rapidly with increasing ω_R (Fig. 10) as expected for a high-order multiphonon process.

(2) At higher fields saturation effects will be exhibited. The onset of saturation effects, determined by Eq. (IV.24), will occur when

$$[\mu_{v,v\pm1}\epsilon]_{OS}\gtrsim |E(n,v\pm1)-E(n,v)| \ . \qquad (V.10)$$

Utilizing Eq. (V.6) we take $(\bar{v}+1)^{1/2}\mu_{01}$ for the highest value of the transition moment between adjacent levels, while from Eq. (V.3) we get $|\Delta-2(\bar{v}+1)x|$ for the energy spacing between adjacent levels. Thus the condition for the onset of saturation effects in the quasidiatomic model is

$$(\bar{v}+1)^{1/2}[\omega_R]_{OS}\gtrsim \Delta E_{\max} \ , \qquad (V.11)$$

where the maximum value of the energy spacing between adjacent levels is

$$\Delta E_{\max}=\Delta, \quad \Delta>0 \text{ and } \Delta/x>2\bar{v}+1 \ ,$$

$$\Delta E_{\max}=(2\bar{v}+1)x-\Delta, \quad \Delta>0 \text{ and } \Delta/x<2\bar{v}+1 \ ,$$

$$\Delta E_{\max}=(2\bar{v}+1)x-\Delta \quad \Delta<0 \ . \qquad (V.12)$$

At even higher fields when $\mu_{v,v\pm1}\epsilon$ exceed the energetic spread $\delta(\Delta)$ of the dressed states, i.e.,

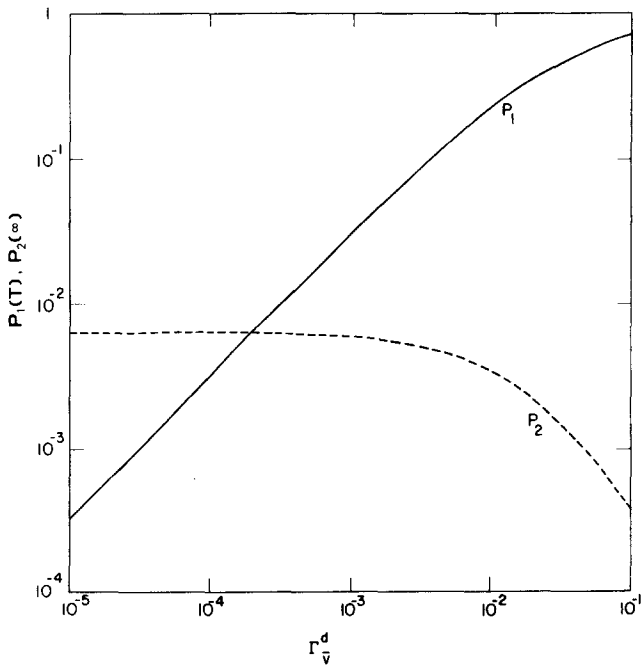

FIG. 6. The dependence of the molecular photodissociation probability $P_1(T)$ during the pulse and the photofragmentation probability $P_2(\infty)$ after the pulse on the decay width $\Gamma_{\bar{v}}^{D}$ of the (single) metastable state. Calculations for the quasidiatomic model with the parameters $M=10$, $\omega_R=10\ \mathrm{cm}^{-1}$, $x=1\ \mathrm{cm}^{-1}$, $\Delta=0$, $T=5\times10^{3}$ cm.

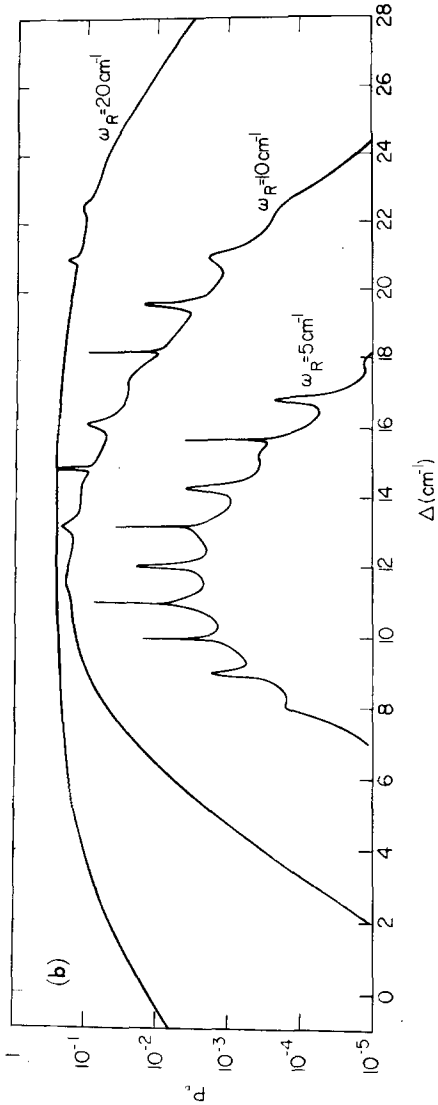

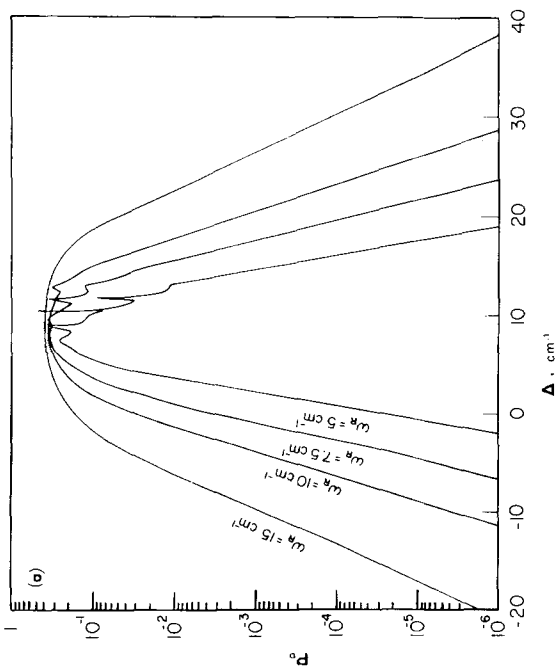

FIG. 7. P_D vs Δ curves at different laser powers for the quasidiatomic model with $x=1$ cm^{-1}, $\Gamma_v^D=10^{-3}$ cm^{-1}, $T=5\times10^3$ cm. (A) $M=10$; (B) $M=15$.

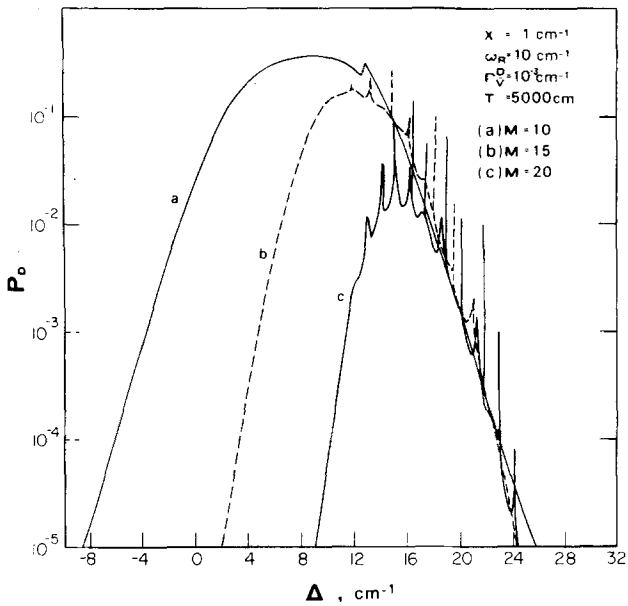

FIG. 8. The dependence of the photodissociation yield in the quasidiatomic model on the number M of levels $\omega_R=10$ cm^{-1}, $x=1$ cm^{-1}, $\Gamma_v^D=10^{-3}$ cm^{-1}, $T=5\times10^3$ cm, $M=10$, 15, and 20, as indicated.

$$(\bar{v}+1)^{1/2}[\omega_R]_{CS} \gtrsim \delta(\Delta) , \tag{V.13}$$

complete saturation occurs. Equations (V.11) and (V.13) together with Eq. (V.5) determine the dependence of the laser field required for the saturation onset and for complete saturation on the off-resonance energy Δ, on the anharmonicity x, and on the number of levels $M=\bar{v}+1$. The lower limits of the field for the onset of saturation is given by

$$[\omega_R]_{OS} = \Delta E_{max}/(\bar{v}+1)^{1/2} , \tag{V.14}$$

while the lower limit for complete saturation is

$$[\omega_R]_{CS} = \delta(\Delta)/(\bar{v}+1)^{1/2} . \tag{V.15}$$

In Fig. 10 we mark these values of $[\omega_R]_{OS}$ and of $[\omega_R]_{CS}$ for a model system where $M=10$, $x=1$ cm^{-1} and where Δ was taken at Δ = 0 and at Δ = 8 cm^{-1} [we note that in the latter case P_D vs Δ reaches its maximum value (Fig. 8)]. The behavior of P_D vs ω_R is just as expected on the basis of Eqs. (V.11), (V.13), and (V.5). From the results portrayed in Figs. 7–9 we note that the saturation onset increases with increasing x and of M, as expected on the basis of Eq. (V.11).

(3) The P_D vs Δ curves are characterized by a maximum at the off-resonance energy $\bar{\Delta}$, which exhibits only a weak dependence on the field strength and which is determined by the number of levels and by the anharmonicity. From Figs. 7–9 we note that $\bar{\Delta}$ is given by

$$\bar{\Delta} = \bar{v}x . \tag{V.16}$$

Thus, maximum photofragmentation efficiency is accomplished in high field when the lowest $v=0$ and the highest $\bar{v}$ level are resonant. As $\bar{\Delta}>0$ anharmonicity effects should be compensated by tuning the laser source below the 0–1 molecular transition in accordance with Bloem-

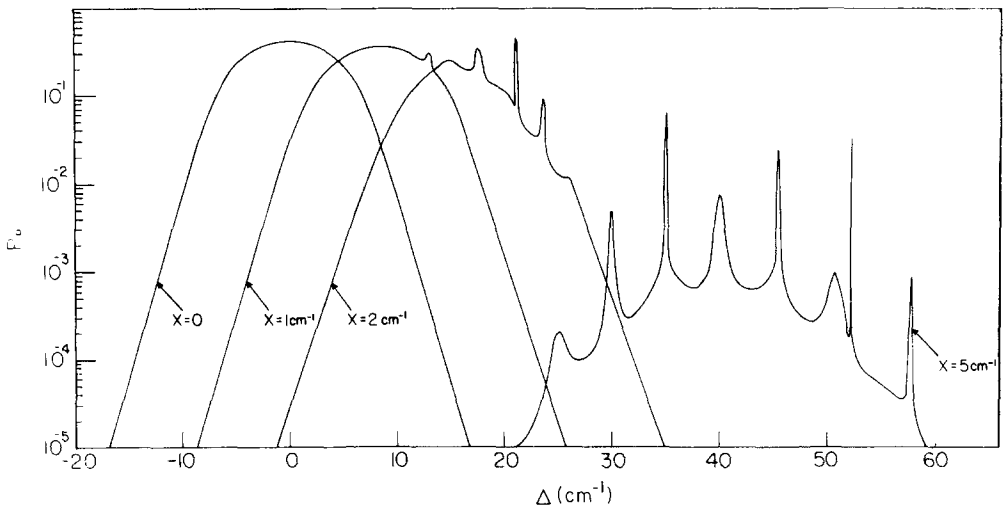

FIG. 9. Effect of anharmonicity on P_D calculated in the quasidiatomic model: $M=10$, $\omega_R=10$ cm^{-1}, $\Gamma_v^D=10^{-3}$, $T=5\times10^3$ cm, $x=0$, 1 cm^{-1}, 2 cm^{-1}, and 5 cm^{-1}, as indicated.

bergen's classical argument.[18] It is of interest to determine the saturation condition at the off-resonance energy $\bar{\Delta}$. In this case we have from Eqs. (V.12) and (V.16) $\Delta E_{\max}=\bar{\Delta}=\bar{v}x$, while Eq. (V.5) leads to $\delta(\bar{\Delta})=\bar{v}^2x/4$. Utilizing Eqs. (V.14) and (V.15) we get

$$[\omega_R]_{OS}\simeq\bar{v}^{1/2}x\,,\qquad \Delta=\bar{\Delta} \tag{V.17a}$$

and

$$[\omega_R]_{CS}\simeq\frac{\bar{v}^{3/2}x}{4}\,,\qquad \Delta=\bar{\Delta}\ . \tag{IV.17b}$$

(4) The P_D vs Δ curve is considerably broadened with increasing ω_R. The same behavior is also exhibited for a truncated harmonic oscillator.[18]

(5) The P_D vs Δ curve is characterized by several regularly spaced sharp resonances superimposed on a broad background. The resonances are prominent at moderately low fields being shifted and broadened at higher ω_R and when $\omega_R\sim\Delta$, the resonances merge into a broad background. The nature of resonances in multiphoton excitation of this multilevel system may be elucidated by examining Fig. 4 where we display the zero-order dressed molecular states for several values of Δ. We note that whenever $\omega_0-\omega=vx$, the vth level is degenerate with the $v=0$ dressed level, (i.e., the $v\to v+1$ transition is in resonance with the laser frequency), resulting in a resonance in the P_D vs Δ curve. We thus expect a series of resonances to be separated by x, which is borne out by our numerical results. Some additional resonances may originate from many other combinations of (zero-order) levels whenever degeneracy is encountered. This effect is of limited interest as rotational effects will probably result in a smearing of these resonances.

(6) The quasidiatomic model exhibits high isotopic selectivity. Vibrational isotope shifts S of a few wavenumbers (Table II) are sufficient to obtain considerable isotopic enrichment in the photofragmentation process. When the isotopic molecular species characterized by the lower molecular frequency ω_0 is excited at $\omega<\omega_0$, then $\Delta>0$ for both isotopic species, and the maximum isotopic separation factor β is[49]

$$\beta=P_D(\bar{\Delta})/P_D(\bar{\Delta}+S)\ . \tag{V.18}$$

Typical numerical results for β are presented in Fig. 11, indicating high isotopic selectivity which, as expected, is reduced by a further increase in the field intensity.

We now address ourselves to the central issue of whether the quasidiatomic model is adequate to account for the experimental observations of multiphoton photofragmentation of polyatomics. To answer this question we turn to some rough numerical estimates of the threshold power required to induce observable photofragmentation and of the power required for the onset of saturation effects. From the numerical data protrayed in Figs. 6–10, we conclude that the threshold for

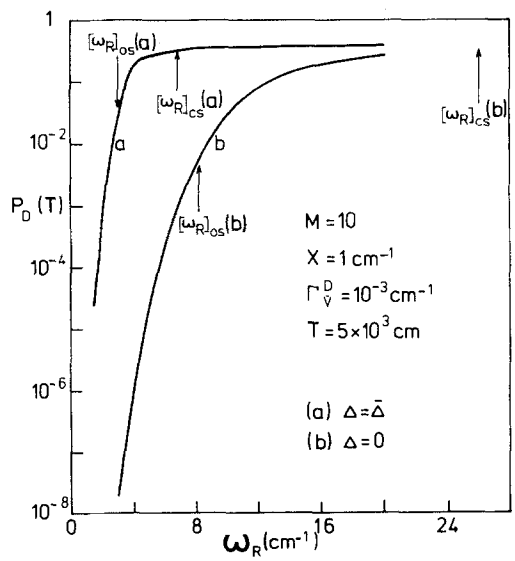

FIG. 10. Model calculations of the photofragmentation probability vs the Rabi frequency ω_R for the quasidiatomic model: $M=10$, $x=1$ cm^{-1}, $\Gamma_v^D=10^{-3}$ cm^{-1}, $T=5\times10^3$ cm. (A) $\Delta=\bar{\Delta}$; (B) $\Delta=0$, the values of $[\omega_R]_{OS}$ and of $[\omega_R]_{CS}$, Eqs. (V.11), (V.13), and (V.17), are indicated by arrows.

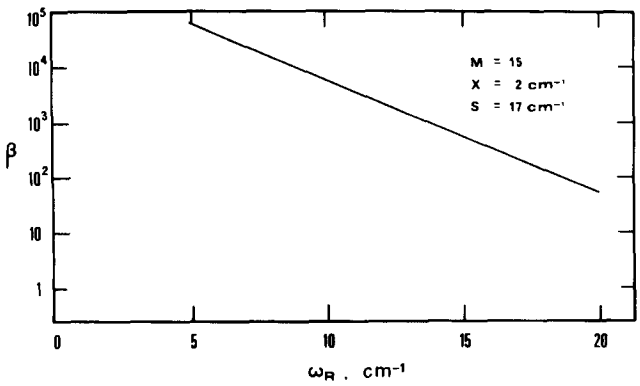

FIG. 11. Model calculations of the isotopic separation factor β, Eq. (V.18), vs the laser field intensity for the quasidiatomic model: $M=15$, $x=2$ cm^{-1}, $\Gamma_{\bar{v}}^{D}=10^{-3}$ cm^{-1}, $T=5\times10^{3}$ cm.

observable photofragmentation, $P_D \sim 10^{-4}$, (per pulse) is obtained at the Rabi frequency $(\omega_R)_t$, which is about 1 order of magnitude lower than $[\omega_R]_{OS}$. Consequently, we define, somewhat arbitrarily, the threshold power at $\Delta = \bar{\Delta}$,

$$(\omega_R)_t \simeq [\omega_R]_{OS}/10 = x\bar{v}^{1/2}/10 \ , \qquad (V.19)$$

where we have made use of Eq. (V.17a). A cursory examination of Eqs. (V.19) and of Eq. (V.17a) reveals that both thresholds depend quite weakly on the number $M=\bar{v}+1$ of the coupled levels and depend linearly on the anharmonicity constant. Now, for a polyatomic molecule we take roughly $\bar{v} \simeq D_e/\omega_0 = 25-30$ (where D_e is the bond dissociation energy) and $x \simeq 2$ cm^{-1} for a "typical" diagonal anharmonicity constant. These "intelligent guesses" yield $(\omega_R)_t \sim 1$ cm^{-1}, which corresponds to a laser power of $I \sim 0.25$ GW cm^{-2} for the threshold, while $[\omega_R]_{OS} \sim 10$ cm^{-1} and a laser power of $I \sim 25$ GW cm^{-2} is required for the onset of saturation effects. This very rough estimate of $[\omega_R]_{OS}$ is somewhat higher than the experimental threshold[14] $I \simeq 1$ GW cm^{-2} for the onset of saturation effects in the photodissociation of BCl_3. The estimate for the threshold power $I \sim 250$ MW cm^{-2} for observable photodissociation considerably exceeds the experimental value[11] of $I \simeq 5-10$ MW cm^{-2} for SF_6. We thus conclude that the quasidiatomic model predicts threshold values for experimentally observable multiphoton photodissociation in the range of ~1 GW cm^{-2}, which are higher than those experimentally observed.

We shall make a slight detour at this stage and consider briefly coherent multiphoton dissociation of diatomics within the framework of the present model. In this case anharmonicity is often higher than the (diagonal) anharmonicity in a nonsymmetric mode of a polyatomic and the corresponding values of $(\omega_R)_t$ and of $[\omega_R]_{OS}$ will be higher. A reasonable estimate for a diatomic can be obtained utilizing the approximate relations for a truncated anharmonic oscillator $x \cong \omega_0^2/4D_e$ and $\bar{v} \cong \omega_0/2x = 2D_e/\omega_0$, so that Eqs. (V.17a) and (V.19) result in

$$[\omega_R]_{OS} \simeq (\omega_0/D_e)^{1/2}(\omega_0/2\sqrt{2}) \ ,$$
$$(\omega_R)_t \simeq (\omega_0^{3/2}/20\sqrt{2}\,D_e) \ . \qquad (V.20)$$

For typical values of $\omega_0 \simeq 1000$ cm^{-1} and $D_e \simeq 30\,000$ cm^{-1} $[\omega_R]_{OS} \simeq 60$ cm^{-1} while $(\omega_R)_t \simeq 6$ cm^{-1}. Thus the threshold for photodissociation of diatomics is expected to occur at laser powers of ~9 GW cm^{-2}. This conclusion is not inconsistent with the recent (yet unpublished) work of the Los Alamos group,[50] who failed to dissociate diatomic molecules in intense laser fields.

The quasidiatomic model requires some further modification. First, the assumption that radiative coupling occurs only between adjacent levels which is valid in Range I has to be relaxed at high energies where the selection rules for the harmonic oscillator, Eq. (V.5), used herein will break down. Second, and more interesting, one should consider physical mechanisms for the compensation of anharmonicity effects, which are responsible for high threshold values obtained for the quasidiatomic model. Larsen and Bloembergen[35] have pointed out that rotational effects, which are neglected in the present treatment, can compensate for anharmonicity effects. Within the framework of the quasidiatomic model such compensation for anharmonicity by transitions between different rotational states will operate in Ranges I, II, and III, leading to a considerable reduction in the power threshold required for observable photodissociation. An alternative physical mechanism, which compensates for anharmonicity effects, involves near-resonance coupling between mixed states in Ranges II and III. We propose that the role of intrastate level mixing exhibited in polyatomics is of crucial importance in the process of multiphoton photodissociation. The consequences of the effects of level scrambling in polyatomic molecules can be accounted for in terms of the two-ladder model which we shall now consider in some detail.

VI. THE TWO-LADDER MODEL

In this model [Model (C), Sec. III] we approximate the molecular levels which are in near resonance with the laser energy $\hbar\omega$ in terms of the two following subsets of states: (a) N_I levels in Range I which correspond to a truncated anharmonic oscillator characterized by a frequency ω_0 and anharmonicity x, and (b) N_{II} levels in Ranges II and III which correspond to mixed states and which are in exact resonance with the laser field. The energies of these $M = N_I + N_{II}$ molecular levels are given by

$$E_\alpha = \omega_0(\alpha-1) - x(\alpha-1)^2, \quad \alpha = 1, 2, \ldots, N_I \ ,$$
$$E_\alpha = E_{\alpha-1} + \omega \ , \quad \alpha = (N_I+1), (N_I+2) \cdots M \ . \qquad (VI.1)$$

The dressed molecular states $E(\alpha, n-\alpha+1)$, Eq. (V.3), are characterized by the energies

$$E(\alpha, n-\alpha+1) = n\omega + (\alpha-1)\Delta - (\alpha-1)^2 x, \quad \alpha = 1 \cdots N_I \ , \qquad (VI.2a)$$
$$E(\alpha, n-\alpha+1) = n\omega + (N_I-1)\Delta - (N_I-1)^2 x \ ,$$
$$\alpha = (N_I+1) \cdots M, \qquad (VI.2b)$$

and the energetic spread is

$$\delta(\Delta) = (\Delta^2/4x) - (N_I-1)\Delta - x(N_I-1)^2 \ , \quad N_I \geq (\Delta/x)+1$$
$$= \Delta^2/4x \quad N_I \leq (\Delta/x)+1 \ , \qquad (VI.3)$$

where the off-resonance energy Δ is defined by Eq. (V.5). As before, we describe the decomposition process by assigning a single molecular state $\alpha = M$ to Range III, which is characterized by the predissociative width Γ_M^D. Next, we consider the radiative coupling terms between adjacent levels. In Region I we approximate these terms by those appropriate for a harmonic oscillator, Eq. (V.6), while in Regions II and III coupling between adjacent levels [Eq. (IV.3)] is assumed; thus, the nonvanishing matrix elements are

$$\langle \alpha, n-\alpha+1 | H_{\rm int} | \alpha+1, n-\alpha \rangle = \mu_{01}\, \alpha^{1/2} \epsilon, \quad \alpha = 1 \cdots N_{\rm I},$$
$$\langle \alpha, n-\alpha+1 | H_{\rm int} | \alpha+1, n-\alpha \rangle = \mu_{\alpha,\alpha+1} \epsilon, \quad \alpha = N_{\rm I}+1 \cdots M. \qquad \text{(VI.4)}$$

Here μ_{01} corresponds to the transition moment for the $v=0 \rightarrow v=1$ transition, which is known from molecular spectroscopy. The radiative coupling terms connecting adjacent mixed levels in Regions II and III are unknown. The breakdown of the harmonic oscillator approximation is expected to be severe in this region. One could, in principle, attempt to expand the mixed states in terms of a (multidimensional) harmonic basis to evaluate the coupling terms $\mu_{\alpha,\alpha+1} (\alpha = N_{\rm I}+1 \cdots M)$. Such a procedure was applied for small polyatomics at moderately low energies.[20a,40] At the present stage of our analysis we shall take these radiative coupling terms in Regions II and III as variable parameters. We shall invoke the reasonable assumption that

$$|\mu_{\alpha,\alpha+1}/\mu_{01}| \leq 1 \qquad \text{(VI.5)}$$

for all $\alpha = (N_{\rm I}+1), \ldots, M$. In our numerical calculations we shall either take all the radiative coupling terms in Regions II and III to be constant or, alternatively, we shall assume that these terms vary randomly with α in the range determined by Condition (VI.5).

The effective Hamiltonian, Eq. (IV.10), for the problem is characterized by the diagonal matrix elements

$$\langle \alpha, n-\alpha+1 | H_{\rm eff} | \alpha, n-\alpha+1 \rangle = E(\alpha, n-\alpha+1), \quad \alpha = 1, 2 \cdots (M-1)$$
$$= E(M, n-M+1) - \tfrac{1}{2} i \Gamma_M^D \quad \alpha = M \qquad \text{(VI.6)}$$

being expressed in terms of Eq. (VI.2). The nonvanishing off-diagonal matrix elements of the effective Hamiltonian are given by Eq. (VI.4). The photofragmentation yield P_D, Eq. (IV.14b), is calculated utilizing Eqs. (IV.11), (IV.12), and (IV.20).

Numerical simulations for the two-ladder model were conducted using the following parameters: $M = 10$, 15, and 20; $N_{\rm I} = 5-M$; $x = 0-10$ cm^{-1}; $\Delta = -50$ cm^{-1} to $+100$ cm^{-1}, $\Gamma_M^D = 10^{-3}$ cm^{-1}; and $T = 5\times10^3$ cm. We have chosen $\Gamma_M^D T \gg 1$, whereupon the dominating contribution to the photofragmentation yield occurs during the pulse. The radiative coupling in Region I was specified in terms of the Rabi frequency $\omega_R = \mu_{01}\epsilon/\hbar$, which was varied in the range $\omega_R = 0.01-10$ cm^{-1}. The $N_{\rm II}$ transition moments $\mu_{\alpha,\alpha+1}$ and the radiative coupling terms $\mu_{\alpha,\alpha+1}\epsilon$ $[\alpha = (N_{\rm I}+1) \cdots M]$ were specified in terms of one of the following procedures:

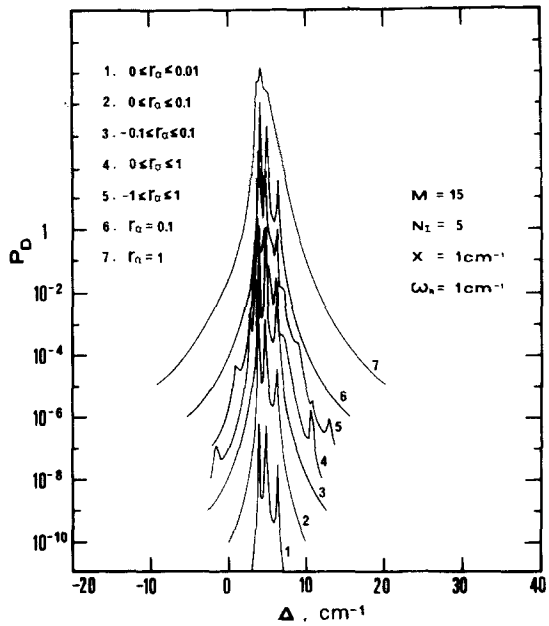

FIG. 12. The dependence of the photodissociation yield in the two-ladder model at moderate laser field on the choices of the transition moments $\mu_{\alpha,\alpha+1} [\alpha = (N_{\rm I}+1) \cdots M]$ in Regions II and III. The $\log_{10} P_D$ scale is given for Curve 1. Each of the other $\log_{10} P_D$ vs Δ curves in this figure which are labeled by $i = 2$, 3, 4, 5, 6, 7 is horizontally displaced upwards by $(i-1)$ units. $M = 15$, $N_{\rm I} = 5$, $x = 1$ cm^{-1}, $\omega_R = 1$ cm^{-1}, $\Gamma_M^D = 10^{-3}$ cm^{-1}, $T = 5\times10^3$ cm. The values of $r_\alpha = \mu_{\alpha,\alpha+1}/\mu_{01}$ are indicated on the figure. A constant value of r_α implies that all transition moments are equal. Otherwise, r_α is a random number in the range shown in each case.

(a) A constant value $\mu_{\alpha,\alpha+1} = r\mu_{01}$, where $r \leq 1$, was assigned to all these transition moments.

(b) The transition moments were assumed to be random but of the same sign. Each transition moment $\mu_{\alpha,\alpha+1}$ was assigned a random number r_α in the range $0 \leq r_\alpha \leq f$, where $0 \leq f \leq 1$. The transition moments are then taken as $\mu_{\alpha,\alpha+1} = r_\alpha \mu_{01}$.

(c) The transition moments were taken to the random. Each transition moment $\mu_{\alpha,\alpha+1}$ was assigned a random number r_α in the range $-f < r_\alpha < +f$, where $0 \leq f \leq 1$, and $\mu_{\alpha,\alpha+1} = r_\alpha \mu_{01}$.

Numerical calculations of the photofragmentation yield were carried out utilizing a coarse graining averaging procedure over time intervals of $\Delta t = 0.3$ nsec, as described in Sec. V. When procedure (b) or (c) for the assignment of the transition moments in Regions II and III were employed, we have attempted to correct for the effects of statistical fluctuations in the P_D data by using different sets of random numbers and averaging the results of P_D at each Δ for 2–4 separate runs. This procedure converges (within 10% or so) after two runs, and additional averaging is not necessary.

We now turn to the results of the numerical simulations for the two-ladder model. The alert reader should recognize that the weakest point of the present treatment involves our ignorance of the transition moments in Regions II and III. Accordingly, we have conducted a series of model calculations (Figs. 12 and 13) exploring

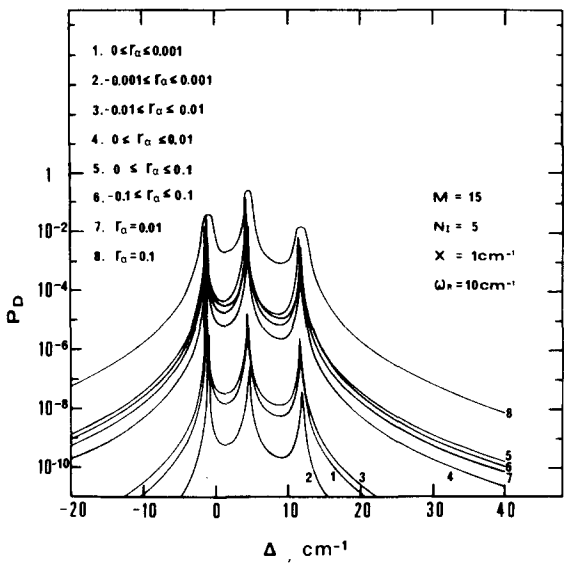

FIG. 13. The dependence of P_D in the two-ladder model at high field on the choice of the transition moments $\mu_{\alpha,\alpha+1}[\alpha = (N_I+1)\cdots M]$ in Regions II and III. $M=15$, $N_I=5$, $x=1$ cm^{-1}, $\omega_R=10$ cm^{-1}, $\Gamma_M^D=10^{-3}$ cm^{-1}, $T=5\times10^3$ cm. The values of r_α used in these calculations are indicated on the figure and labeled as in Fig. 12.

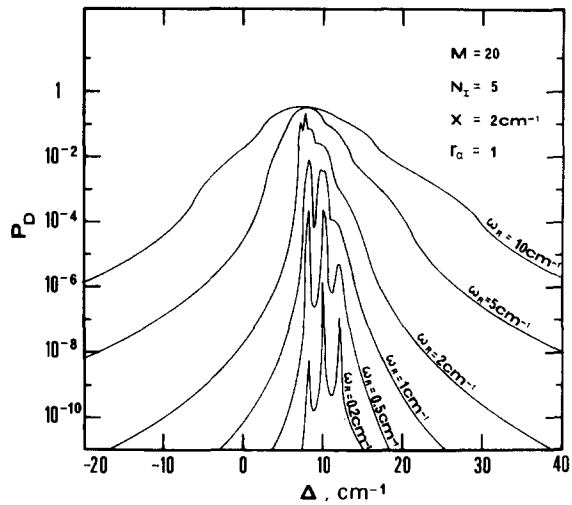

FIG. 15. Model calculations of field effects on P_D for the two-ladder model. $M=20$, $N_I=5$, $x=2$ cm^{-1}, $\Gamma_M^D=10^{-3}$ cm^{-1}, $T=5\times10^3$ cm, $\mu_{\alpha,\alpha+1}=\mu_{01}$ for all $\alpha=(N_I+1)\cdots M$. Laser intensity is specified in terms of the Rabi frequency ω_R.

the dependence of P_D on $r_\alpha=\mu_{\alpha,\alpha+1}/\mu_{01}$, where r_α was chosen either as a constant or as a random number which is varied in the range 0 to f or $-f$ to $+f$, according to the recipes previously outlined. From Figs. 11 and 12 several conclusions emerge. First, when r_α is chosen to be random, then for $f\leq0.1$, P_D exhibits quite a marked dependence on f, and increases with increasing f, as expected. Second, for random r_α with $f\leq0.1$, P_D is larger by about 1 order of magnitude when all the transition moments in Region II are characterized by the same sign, i.e., $0\leq r_\alpha\leq f$, relative to the case when both the magnitudes and the signs of the transition moments are random, i.e., $-f\leq r_\alpha\leq f$. Third, when $f\geq0.1$, the maxima of the photodissociation yields vs Δ calculated according to procedures (a), (b), and (c) are practically identical. In what follows we shall choose either $r\geq0.1$, when procedure (a) will be applied, or $f\geq0.1$, when procedure (b) or (c) will be utilized. We now turn to field effects and saturation phenomena. In Figs. 14–16 we present some typical results for $M=15$ and $M=20$ with $N_I=5$, which exhibits the following characteristics:

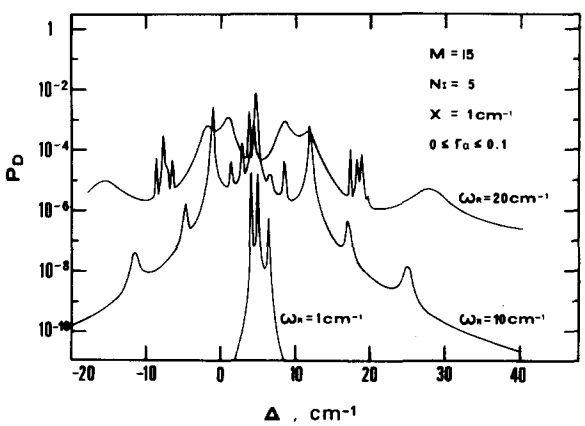

FIG. 14. Model calculations of field effects on P_D for the two-ladder model. $M=15$, $N_I=5$, $x=1$ cm^{-1}, $\Gamma_M^D=10^{-3}$ cm^{-1}, $T=5\times10^3$ cm, $\mu_{\alpha,\alpha+1}=r_\alpha\mu_{01}$ (where $0\leq r_\alpha\leq1$). Laser intensity is specified in terms of the Rabi frequency ω_R.

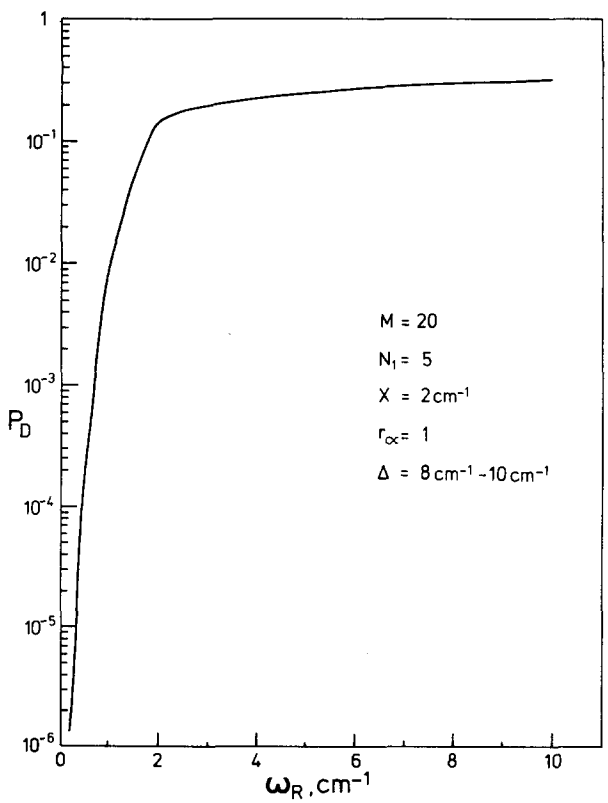

FIG. 16. The dependence of P_D on the laser intensity, ω_R, at $\Delta=\bar{\Delta}$, i.e., at maximum photodissociation probability, ignoring the effects of resonances for the two-ladder model. Molecular and laser parameters same as those in Fig. 15.

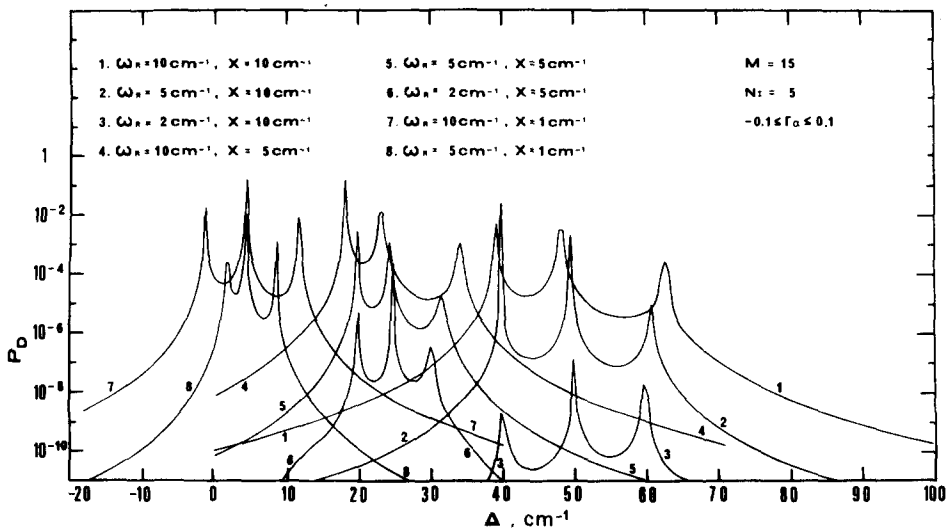

FIG. 17. The dependence of P_D on the diagonal anharmonicity constant x, in the two-ladder model. $M=15$, $N_I=5$, $-0.1 \leq r_\alpha \leq 0.1$. ω_R was varied in the range 2–10 cm^{-1} while x was varied in the range 1–10 cm^{-1}, as indicated on the figure.

(1) A fast increase of P_D vs ω_R for "low" fields, $\omega_R \lesssim 1$ cm^{-1} for all Δ.

(2) At the maximum of P_D vs Δ, the onset of saturation for moderate values of the anharmonicity ($x=1$–2 cm^{-1}) is exhibited for $\omega_R \sim 1$–2 cm^{-1}, while for $\omega_R \geq 2$ cm^{-1} complete saturation occurs.

(3) The P_D vs Δ curves broaden considerably with increasing Δ. We note that all these features are qualitatively similar to those encountered in the quasidiatomic model (Sec. V) except that the onset of saturation now occurs for a somewhat lower field. Next, we consider anharmonicity effects, and from the results summarized in Figs. 17–19 we conclude that (i) The P_D vs Δ curves are now characterized by a maximum at the off-resonance energy

$$\bar{\Delta} = (N_I - 1)x \quad . \tag{VI.7}$$

The maximum efficiency now occurs when the lowest dressed level is in resonance with the N_I dressed level, while in the quasidiatomic model the maximum efficiency is exhibited when the $v=0$ dressed level is in resonance with the M level. As in the case of the quasidiatomic model, $\bar{\Delta} \geq 0$, as anharmonicity effects in Region I have to be compensated. $\bar{\Delta}$ is practically independent of the field and for constant N_I $\bar{\Delta}$ is independent of M. (ii) A rich resonance structure is exhibited in the P_D vs Δ curves. For moderate fields or for high anharmonicity ($x \sim 10$ cm^{-1}), regularly spaced resonances are observed whenever degeneracy occurs between the lowest level and any other dressed level of the anharmonic ladder in Region I. These regularly spaced resonances are then just split by the anharmonicity constant x. At high fields these regularly spaced resonances originating from Re-

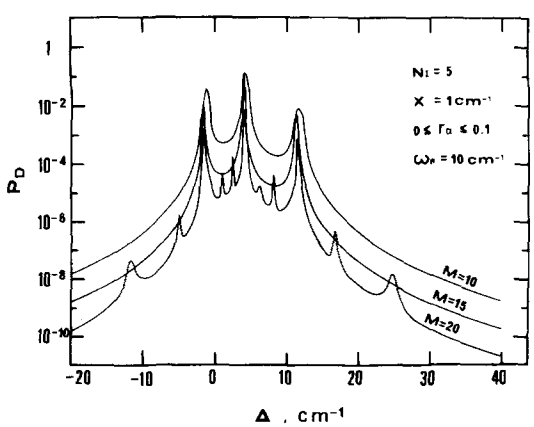

FIG. 18. The dependence of P_D in the two-ladder model on the total number of levels. $M=10$, 15, 20; $N_I=5$, $x=1$ cm^{-1}, $0 \leq r_\alpha \leq 0.1$, $\omega_R=10$ cm^{-1}.

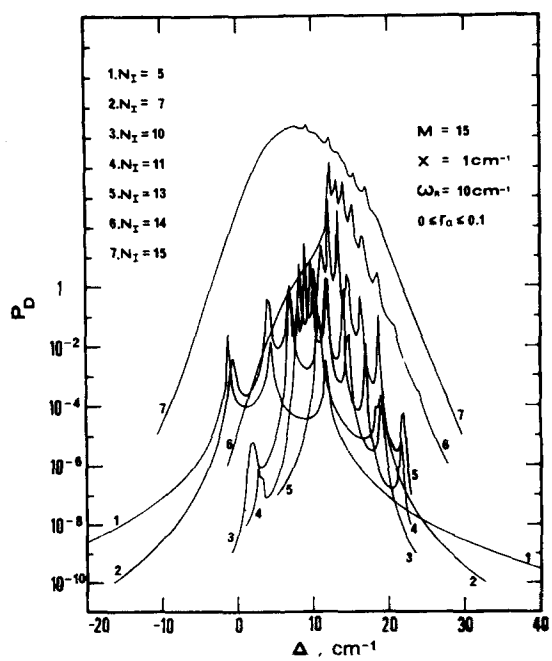

FIG. 19. Model calculations of the effect of changing the number N_I of levels in Region I (at constant M) on the P_D vs Δ yield curves for the two-ladder model. $M=15$, $N_I=5$–15, $x=1$ cm^{-1}, $\omega_R=10$ cm^{-1}, $0 \leq r_\alpha \leq 0.1$. The $\log_{10}P_D$ scale is given for Curve 1. Each of the other $\log_{10}P_D$ vs Δ curves in this figure which are labeled by $i=2$, 3, 4, 5, 6, 7 is horizontally displaced upwards by $(i-1)$ units.

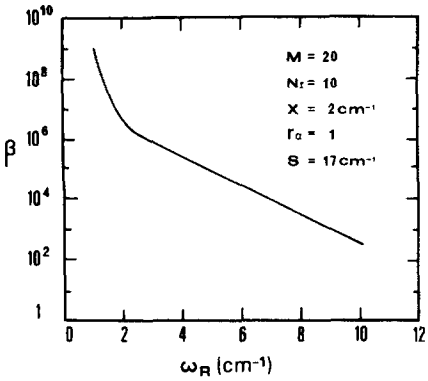

FIG. 20. Model calculations of the isotopic separation factor β, Eq. (V.18), vs the laser field intensity for the two-ladder model.

gion I are smeared out, as in the case of the quasidiatomic model. However, when the transition moments in Region II are random, an additional resonance structure is observed at high fields, which originates from Stark shifts of the levels in Region II (see Fig. 17). Again, we expect that rotational effects may erode the resonance structure. (iii) The dependence of P_D on ω_R is weak (Fig. 16) in contrast to the features of the quasidiatomic model. (iv) The two-ladder model exhibits high isotopic selectivity for reasonably high values of the vibrational isotopic shift as appropriate for SF_6 (Fig. 20). These results are similar to those observed for the quasidiatomic model (see Fig. 11). We thus conclude that isotopic selectivity in both models originates from selective radiative coupling in Region I.

We now proceed to discuss some physical features of the two-ladder model.

A. Saturation effects

The conditions for the onset of saturation at $\Delta = \bar{\Delta}$ are given by Eqs. (IV.24) and (IV.25). Condition (IV.25) regarding the decay width

$$\mu_{M-1,M}\epsilon \gtrsim \Gamma_M^D \qquad \text{(VI.8)}$$

is expected to be satisfied for the laser fields with which we are concerned (i.e., $\omega_R \gtrsim 0.1$ cm^{-1}, $f \geq 0.1$), and we have to focus attention on the energetic condition (IV.24). Now, as the states in Region II are in resonance, we have just to discuss saturation effects in Region I. Considering the radiative coupling between the highest states in Region I, we get for the onset of saturation

$$[\mu_{N_I-1,N_I}\epsilon]_{OS} \simeq |E(N_I-1) - E(N_I)| \ , \qquad \text{(VI.9)}$$

where $E(\alpha) \equiv E(\alpha, n-\alpha+1)$. Making use of Eq. (V.6) for the transition moment and Eq. (VI.2a) for the energy levels, we obtain for the maximum of the photodissociation yield

$$[\omega_R]_{OS} \simeq (N_I+2)(N_I)^{-1/2}x \sim (N_I)^{1/2}x \qquad \text{(VI.10)}$$

at $\Delta = \bar{\Delta}$. The threshold for complete saturation is obtained from Eq. (IV.26). As Condition (VI.8) is expected to hold, we get for complete saturation

$$[\mu_{N_I-1,N_I}\epsilon]_{CS} \simeq \delta(\Delta) \ . \qquad \text{(VI.11)}$$

Utilizing Eqs. (V.6), (VI.3), and (VI.7), we obtain

$$[\omega_R]_{CS} \simeq N_I^{3/4}x/4 \ , \quad \Delta = \bar{\Delta} \ . \qquad \text{(VI.12)}$$

A cursory examination of Eqs. (VI.10) and (VI.12) for the two-ladder model when confronted with Eq. (V.17) for the quasidiatomic model reveals that both onsets are appreciably lower in the former case. $[\omega_R]_{OS}$ is reduced by $(N_I/M)^{1/2}$, while $[\omega_R]_{CS}$ is lowered by $(N_I/M)^{3/2}$, where $M \sim (D_e/\omega_0) - (2D_e/\omega_0)$ is the effective total member of levels in the quasidiatomic model. To provide a rough numerical estimate for these onset powers in the two-ladder model, we take $N_I = 5$ and $x = 2$ cm^{-1}, whereupon Eqs. (VI.10) and (VI.12) yield $[\omega_R]_{OS} \sim [\omega_R] \sim 4$ cm^{-1}, a result compatible with the numerical data of Fig. 14. This onset for saturation which corresponds to the laser power of $I \simeq 4$ GW cm^{-2} is compatible with the experimental onset of saturation effects at $I \simeq 1$ GW cm^{-2} reported[14] for the photofragmentation of BCl_3. It is important to note that in the two-ladder model for moderate values of $N_I \lesssim 5$, $[\omega_R]_{OS} \sim [\omega_R]_{CS}$ and the onset of saturation effects is abrupt. We would like also to point out that near saturation P_D is independent of the total number of levels $M = D_e/\omega_0$ in the present model provided that Eq. (VI.8) holds. This conclusion concurs with the numerical results of Fig. 16.

B. Threshold power for observable photofragmentation

This experimental threshold for which $P_D \sim 10^{-4}$–10^{-5} is roughly estimated, as in Sec. V, to be $(\omega_R)_t \sim [\omega_R]_{OS}/10$, so that

$$(\omega_R)_t \sim (N_I)^{1/2}x/10 \ , \quad \Delta = \bar{\Delta} \ , \qquad \text{(VI.13)}$$

where we have made use of Eq. (VI.10). This experimental threshold exhibits a linear dependence on the diagonal anharmonicity constant x, a weak dependence on N_I, and is practically independent of the total number of levels $M = D_e/\omega_0$. Setting $x = 2$ cm^{-1} and $N_I = 5$, Eq. (VI.13) results in $(\omega_R)_t \sim 0.4$ cm^{-1}, which corresponds to a laser power of $I = 40$ MW cm^{-2} (for $\mu_{01} = 0.1$ D). This estimate of $(\omega_R)_t$ is still higher by about 1 order of magnitude than the experimentally reported onset of $I = 5$–10 MW cm^{-2} for the photofragmentation of SF_6. The present estimate of $(\omega_R)_t$ disregards rotational effects[35] which will further compensate for anharmonicity defects in Region I.

C. Dependence of the threshold and of the onset for saturation on molecular parameters

When anharmonicity effects are properly compensated by choosing $\Delta \cong \bar{\Delta}$, Eq. (VI.7), the threshold field and the fields required for saturation, i.e., $(\omega_R)_t$, $[\omega_R]_{OS}$, and $[\omega_R]_{CS}$, are determined by the molecular parameters x and N_I but not by M. The linear dependence of the power on the diagonal anharmonicity is self-evident as it relates to the effectiveness in climbing the anharmonic ladder in Region I. The dependence of $(\omega_R)_t$ and $[\omega_R]_{OS}$ on $(N_I)^{1/2}$ and of $[\omega_R]_{CS}$ on $N_I^{3/2}$ establishes a relation between field effects and the molecular level structure. The termination of Region I will occur when the density of background states $\rho_b(E_b)$ is sufficiently large so that Condition (II.6) is obeyed and the effects of level scrambling set in. We thus expect that, in general, N_I

will decrease with increasing of the number of vibrational degrees of freedom. Thus the photodissociation yield (at constant laser power) will increase with increasing of the size of the molecule. In this context it is also of interest to recall that the onset of saturation effects is abrupt for moderate values of $N_I \lesssim 5$. We expect that such an abrupt onset will be observed in molecules where N_I is low, i.e., where the density of the background states is already large at ~ 5000 cm^{-1} above the electronic origin of the ground state. A careful experimental study of the onset of saturation effects under coherent optical excitation of an "isolated" molecule will be of considerable interest. Finally, we would like to note that the threshold power for observable photofragmentation, as well as the field required for saturation, are practically independent of $M = D_e/\omega_0$, i.e., on the bond dissociation energy. This negative conclusion is of considerable importance as for moderate fields which satisfy Condition (VI.8) the molecule can be coherently pumped via resonance coupling in Region II up to the onset of (vibrational or rotational) predissociation on the ground state potential surface. Furthermore, when interstate nonadiabatic coupling is incorporated resonance coupling in Range II can occur to higher excited electronic configurations which can result in electronically excited fragments and even ionic species.

D. Dissociation probability vs laser frequency

Recent, as yet unpublished, work by Lethokov and colleagues[51] provides a confirmation of the general features of the P_D vs Δ curves predicted by the two-ladder model. Multiphoton photodissociation of SF_6 at 0.12 torr at 300 K by a single high-power pulsed CO_2 laser (output 2 J in 90 nsec) resulted in a broad P_D vs Δ distribution peaking at $\bar{\Delta} = 9$ cm^{-1}. This result is consistent with the theoretical prediction provided by Eq. (VI.7). Excitation by two time-delayed, frequency-shifted lasers resulted in a drastic reduction of $\bar{\Delta}$ to the value of $\bar{\Delta} \sim 3$ cm^{-1} and to the narrowing of the P_D vs Δ distribution, as in this case the number N_I of the steps in the first ladder in Region I is reduced.

VII. CONCLUDING REMARKS

The two-ladder model has many attractive features, providing a self-consistent physical picture of how a single polyatomic molecule can overcome anharmonic defects during the high-order multiphoton absorption process. The major mechanism which compensates for anharmonicity effects involves, in our opinion, intrastate anharmonic scrambling in Regions II and III. We have argued that intrastate mixing is of central importance, while the effects of IVR and vibrational energy redistribution within a single molecule are of minor importance. This cardinal point rests on the careful distinction that has to be made between level mixing and IVR. The Condition (II.6) for intrastate coupling sets in at lower energies than the validity Condition (II.8) for IVR. In the energy region $E \gtrsim \bar{E}_b$ the zero-order $\{|v\rangle\}$ states already lose their identity and we argue that the radiative coupling between adjacent $\{|m\rangle\}$ levels separated by ω in the energy region $\bar{E}_b < E < \check{E}_b$ is effective. Thus, when the energy $\check{E}_b$ is reached, the anharmonic coupling terms $V_a(E_b > \check{E}_b)$ are already sufficiently small so that the IVR rate, Eq. (II.9), is negligible on the relevant time scale. Furthermore, the $|v\rangle$ character of the mixed $\{|m\rangle\}$ states, which are in resonance with the laser field, is already small in the high-energy region $E_b \gtrsim \check{E}_b$ of Region II, and we cannot consider a single metastable $|v\rangle$ state "selected" by radiative coupling with a lower level, whereupon the concept of IVR loses its significance.

The two-ladder model is admittedly oversimplified, as in our treatment we had to single out a single state from the manifold of the mixed $\{|m\rangle\}$ levels in each energy range in Regions II and III, which is in resonance with the laser field. A pedantic treatment of the problem would involve the replacement of each of the nonvanishing diagonal and off-diagonal matrix elements of the effective Hamiltonian in Regions II and III by a matrix, but this is not a practical approach. We believe, however, that the two-ladder model elucidates the gross features[52] of coherent multiphoton excitation and photofragmentation of a single "collision-free" polyatomic molecule and provides a set of theoretical predictions which can be confronted with experiment.

ACKNOWLEDGMENTS

We are indebted to Professor A. Ben-Reuven and Professor A. Nitzan for many stimulating discussions.

*Present address: Chemistry Dept., M.I.T., Cambridge, MA 02139.

[1](a) V. S. Letokhov, Science 180, 451 (1973); (b) C. B. Moore, Acc. Chem. Res. 6, 323 (1973); (c) E. Weitz and G. Flynn, Ann. Rev. Phys. Chem. 25, 275 (1974); (d) "High Energy Visible and Ultraviolet Lasers," Tech. Rep. JSR-74-1, Stanford Research Institute, 1975.
[2]M. I. Buchwald, R. Mcfarlane, and S. H. Bauer, Internal Rep., Cornell University, LPS 104, 1972.
[3]N. G. Basov, E. P. Markin, A. N. Oraevskii, A. V. Pankratov, and A. N. Skachkov, JETP Lett. 14, 165 (1972).
[4]V. S. Letokhov and A. A. Makarov, Sov. Phys.-JETP 36, 1091 (1973).
[5](a) B. F. Gordiets, I. A. Osipov, and V. Ya. Panchenko, Sov. Phys.-JETP 38, 443 (1974); (b) B. F. Gordiets, Sh. S. Mamedov and L. A. Shelepin, Sov. Phys.-JETP 40, 640 (1975).
[6]Yu. V. Afanasev, E. M. Belevov, E. P. Markin, and I. A. Poluektov, JETP Lett. 13, 331 (1971).
[7]J. L. Lyman and R. J. Jensen, Chem. Phys. Lett. 13, 421 (1972).
[8]N. R. Isenor, V. Merchant, R. S. Hallsworth, and M. C. Richardson, Can. J. Phys. 51, 1281 (1973).
[9](a) R. V. Ambartsumyan, V. S. Letokhov, E. A. Ryabov, and N. V. Chekalin, JETP Lett. 20, 273 (1975); (b) R. V. Ambartsumyan, Yu. A. Gorkhov, V. S. Letokhov, and G. N. Makarov, JETP Lett. 21, 171 (1975).
[10](a) R. V. Ambartzumian, N. V. Chekalin, V. S. Letokhov, and E. A. Ryabov, Chem. Phys. Lett. 36, 301 (1975); (b) V. Ambartzumian, N. V. Chekalin, V. S. Doljikov, V. S. Letokhov, and E. A. Ryabov, Chem. Phys. Lett. 25, 515 (1974).
[11]J. L. Lyman, R. J. Jensen, J. Rink, C. P. Robinson, and S. D. Rockwood, Appl. Phys. Lett. 27, 87 (1975).
[12]C. P. Robinson, Proc. 2nd Laser Spectrosc. Conf., Megeve (1975).
[13]N. V. Karlov, Yu. N. Petrov, A. M. Prokhorov, and O. M. Stl'makh, JETP Lett. 11, 135 (1970).

[14]S. D. Rockwood, Chem. Phys. 10, 453 (1975).
[15]This is a rough estimate based on the bond energy D_e, obtained from thermochemical data, whereupon the order N of the multiphoton process is $N \cong D_e/\hbar\omega_0$, where $\hbar\omega_0$ is the laser energy.
[16]N. Bloembergen, Opt. Commun. 15, 416 (1975).
[17]G. Herzberg, *Spectra of Polyatomic Molecules* (Van Nostrand, Toronto, 1966).
[18](a) G. J. Pert, J. Quant. Elect. 9, 435 (1973); (b) For a recent perturbative treatment see F. H. M. Faisal, Opt. Commun. 17, 247 (1976).
[19](a) M. F. Goodman and E. Thiele, Phys. Rev. A 5, 1358 (1972); (b) J. Stone, E. Thiele, and M. F. Goodman, J. Chem. Phys. 59, 2909 (1973); *ibid.* 63, 2936 (1975); (c) M. F. Goodman, J. Stone, and E. Thiele, J. Chem. Phys. 59, 2919 (1973); *ibid.* 63, 2929 (1975).
[20](a) S. Nordholm and S. A. Rice, J. Chem. Phys. 61, 203, 768 (1974); (b) R. K. Sander, B. Soep, and R. N. Zare, J. Chem. Phys. 64, 1242 (1976).
[21](a) M. H. Hui and S. A. Rice, J. Chem. Phys. 61, 833 (1974); (b) J. C. Hemminger and E. K. C. Lee, *ibid.* 56, 5284 (1972); (c) G. A. Aniansson, R. P. Creaser, W. H. Held, L. Holmold, and J. P. Toennies, J. Chem. Phys. 61, 5381 (1974); (d) The evidence that intramolecular level distribution in some bimolecular reactions in molecular beams is not statistical [Refs. 21(a), (b)] is not conclusive, as R. A. Marcus (private communication) has pointed out that not all vibrational degrees of freedom have been considered in the former analysis.
[22]A. Lee, R. Le Roy, F. Herman, R. Wolfgang, and J. C. Tully Chem. Phys. Lett. 12, 569 (1972); S. E. Butrill, J. Chem. Phys. 61, 619 (1974).
[23]J. G. Moehlmann, J. T. Gleaves, J. W. Hudgens, and J. D. McDonald, J. Chem. Phys. 60, 2040 (1974).
[24]R. V. Ambartzumian, N. V. Chekalin, Yu. A. Gorkhov, V. S. Letokhov, G. N. Niakarov, and E. A. Ryabov, in *Laser Spectroscopy*, edited by S. Haroche, J. C. Peboy Peyroula, T. W. Hansch, and S. E. Harris (Springer, Heidelberg, 1975), p. 121.
[25](a) A. E. Douglas, J. Chem. Phys. 45, 1007 (1966); (b) M. Bixon and J. Jortner, J. Chem. Phys. 50, 3284 (1969).
[26](a) J. Jortner and R. S. Berry, J. Chem. Phys. 48, 2757 (1968); (b) J. Jortner and S. Mukamel, in *The World of Quantum Chemistry*, edited by R. Daudel and B. Pullman (Reidel, Amsterdam, 1973), p. 145; (c) J. Jortner and S. Mukamel, in *International Review of Science*, Phys. Chem. Ser. Two, Vol. 1, Theoretical Chemistry, edited by A. D. Buckingham and C. A. Coulson (Butterworths, London, 1975), p. 391.
[27]F. H. Mies and M. Kruass, J. Chem. Phys. 45, 4455 (1966).
[28]S. Haroche, Ann. Phys. (Paris) 6, 189 (1971).
[29]M. Sargent, M. Scully, and W. Lamb, in *Laser Physics* (Addison Wesley, Reading, MA, 1974).
[30](a) I. Rabi, Phys. Rev. 49, 324 (1936); (b) J. Rabi, Phys. Rev. 51, 652 (1937).
[31]R. Karplus and J. Schwinger, Phys. Rev. 123, 25 (1961).
[32]L. Mower, Phys. Rev. 142, 799 (1966).
[33]C. Cohen Tannoudji, in *Cargese Lectures in Physics* (Gordon and Breach, London, 1967), Vol. 2.
[34]S. Mukamel and J. Jortner, Chem. Phys. Lett. 40, 150 (1976).
[35]D. W. Larsen and N. Bloembergen, Opt. Commun. 17, 254 (1976). Receipt of a preprint of this paper from Professor N. Bloembergen is gratefully acknowledged.
[36]M. A. Pariseau, I. Suzuki, and J. Overend, J. Chem. Phys. 42, 2355 (1965).
[37]K. Machidz and J. Overend, J. Chem. Phys. 50, 4429, 4437 (1969).
[38]I. M. Mills, in *Molecular Spectroscopy, Modern Research*, edited by K. N. Rao and C. W. Mathews (Academic, New York, 1970), p. 115.
[39]A. R. Hoy, I. M. Mills, and G. Strey, Mol. Phys. 24, 1265 (1972).
[40]R. J. Whitehead and N. C. Handy, J. Mol. Spectrosc. 55, 356 (1975).
[41](a) H. H. Nielsen, Rev. Mod. Phys. 23, 90 (1951); (b) H. H. Nielson, in *Handbook der Physik* (Springer, Berlin, 1959), Vol. 36.
[42]J. Jortner and S. Mukamel (unpublished results). Note that the zero-order states $\{|v\rangle\}$ are not harmonic oscillator wavefunctions but rather eigenstates of Eq. (II.2), while the zero-order states $\{|b\rangle\}$ diagonalize the nuclear Hamiltonian [Eq. (II.1)] and $V_A(E_b) \equiv \langle b|V_A|v\rangle$.
[43]D. Jackson, Los Alamos Report 6025-MS, 1975.
[44]A. Nitzan and J. Jortner, J. Chem. Phys. 56, 5200 (1972).
[45]E. C. Lim and S. Okajima, Chem. Phys. Lett. 37, 403 (1976).
[46](a) P. J. Robinson and K. A. Halbrook, in *Unimolecular Reactions* (Wiley, New York, 1972); (b) W. Frost, in *Theory of Unimolecular Reactions* (Academic, New York, 1973).
[47]W. Louisell, in *Radiation and Noise in Quantum Electronics* (McGraw-Hill, New York, 1964).
[48](a) B. R. Mollow, Phys. Rev. 188, 75 (1969); (b) S. Swain, J. Phys. B 8, L437 (1975).
[49]Equation (V.18) provides an upper limit for β, as averaging over rotational distribution has to be performed. The small isotope effect on the anharmonicity constant x and possible isotope effect on the decay widths have been disregarded.
[50]See Ref. 16.
[51](a) V. S. Lethokov, Paper presented at Conf. Laser Induced Chem., Steambort Springs, CO, 1976. Summarized in Laser Focus, April (1976), p. 12; (b) For a closely related recent discussion of the "leaking" from Range I to Range II, see V. S. Lethokov and A. A. Markov, Opt. Commun. 17, 250 (1976).
[52]During the preparation of this manuscript, papers on closely related subject matter were presented by Ambartzumian, by Rockwood, by Kompa, and by Bloembergen, Cantrell, and Larsen at the International Conference on Tunable Lasers, Loen, Norway, June 1976 [*Proceedings of the International Conference on Tunable Lasers*, edited by A. Mooradian (Springer, Heidelberg, to be published)]. Related papers were also presented at the XIth International Conference on Quantum Electronics, Amsterdam, 1976. (Abstracts of these papers were published in the July 1976 issue of Opt. Commun.) New experimental results, which were not available during the preparation of this paper, may modify some details of the discussion.